

Tracking the Persistence of Harmonic Chains: Barcode and Stability

Tao Hou,^{*} Salman Parsa,[†] Bei Wang[‡]

December 23, 2024

Abstract

The persistence barcode is a topological descriptor of data that plays a fundamental role in topological data analysis. Given a filtration of data, the persistence barcode tracks the evolution of its homology groups. In this paper, we introduce a new type of barcode, called the harmonic chain barcode, which tracks the evolution of harmonic chains. In addition, we show that the harmonic chain barcode is stable. Given a filtration of a simplicial complex of size m , we present an algorithm to compute its harmonic chain barcode in $O(m^3)$ time. Consequently, the harmonic chain barcode can enrich the family of topological descriptors in applications where a persistence barcode is applicable, such as feature vectorization and machine learning.

1 Introduction

There are two primary tasks in topological data analysis (TDA) [27, 30, 53]: reconstruction and inference. In a typical TDA pipeline, the data is given as a point cloud in \mathbb{R}^N . A “geometric shape” K in \mathbb{R}^N is reconstructed from the point cloud, usually as a simplicial complex, and K is taken to represent the (unknown) space X from which the data is sampled. X is then studied using K as a surrogate for properties that are invariant under invertible mappings (technically, homeomorphisms). The deduced “topological shape” is not specific to the complex K or the space X , but is a feature of the homeomorphism type of K or X . For example, a standard round circle has the same topological shape as any closed loop such as a knot in the Euclidean space. Although topological properties of X alone are not sufficient to reconstruct X exactly, they are among a few global features of X that can be inferred from the data sampled from X .

An (ordinary) persistence barcode [10, 31] (or equivalently, a persistence diagram [14, 19, 29]) captures the evolution of homological features in a filtration constructed from a simplicial complex K . It consists of a multi-set of intervals in the extended real line, where the start and end points of an interval (i.e., a bar) are the birth and death times of a homological feature in the filtration. Equivalently, a persistence diagram is a multi-set of points in the extended plane, where a point in the persistence diagram encodes the birth and death time of a homological feature.

A main drawback of ordinary persistent homology is that it does not provide canonical choices of geometric representatives for each bar in the barcode. Specifically, there are two levels of choices in assigning representatives for bars in a persistence barcode: first, we choose a basis for persistent homology in a consistent way across the filtration; second, we choose a cycle representative inside each homology class in the basis. Both levels of choices involve choosing among significantly distinct geometric features of data to represent the same bar in the barcode. Since such choices are not canonical, it can be challenging to interpret their underlying geometric meaning. In addition, while existing works [7, 25, 51] compute optimal representatives for ordinary persistence, the optimality would rely on a choice of weights for the simplices and on the optimality criterion, leading to different shapes. Moreover, computing the optimal representatives is NP-hard in many interesting situations [17, 11, 12, 5, 32, 25].

^{*}University of Oregon, taohou@uoregon.edu

[†]DePaul University, s.parsa@depaul.edu

[‡]University of Utah, beiwang@sci.utah.edu

As our first contribution, we introduce a new type of barcode called *harmonic chain barcode*. This barcode is obtained by tracking the birth and death of harmonic chains in an increasing filtration. Since there is always a *unique* harmonic chain in a homology class, the *harmonic representatives* in our harmonic chain barcode immediately remove the second level of choices in a natural way. The main idea is to take the harmonic chain groups along an increasing filtration, and to observe that the groups grow or shrink due to the birth and death of harmonic chains, resulting in a zigzag module with inclusion maps. Like any zigzag module [8], the module of harmonic chain groups decomposes into interval modules, which then form the harmonic chain barcode. Moreover, since the maps in this zigzag module are essentially inclusions, each representative for a bar in our harmonic chain barcode consists of a single harmonic chain which is alive over the entire bar. We emphasize that our harmonic chain barcode is distinct from the ordinary persistence barcode; see for example Figs. 1 and 2.

The ordinary persistence barcode is shown to be stable [19], which is crucial for applications. The stability means that small changes in the data imply only small changes in the barcode. For our second contribution, we show that our harmonic chain barcode is also stable in the same sense as the stability of persistence barcode [19].

Finally, we present an algorithm for computing the harmonic chain barcode in $O(m^3)$ time for a filtration of size m , matching the complexity of practical algorithms for ordinary persistence.

The interpretation of homological features is crucial for applications such as extracting hierarchical structures of amorphous solids [37] and quantifying the growing branching architectures of plants [42]. Such an interpretation is closely related to the existence of canonical chain representatives for a barcode. In our harmonic chain barcode, using orthogonality, each bar enjoys a canonical choice of representative (within a homology class) which *lives exactly at the time-interval of the bar*. This arguably promises a more interpretable data feature. Therefore, we expect our harmonic chain barcodes to enrich the family of topological descriptors in applications where ordinary persistence barcode is used, such as feature vectorization and machine learning. Note that just from the fact that our barcode is different from the ordinary persistence one cannot argue in favor or against our suggested barcode. Such a comparison is only meaningful in a specific domain of application and when performed using experimental evaluations. We refer to [35] for an interesting pipeline of data analysis using extra properties of harmonic chains. [35] also contains a method of propagating the information from harmonic chains back to original data points which we find also relevant to our harmonic representatives.

2 Related Work

Harmonic chains were first studied in the context of functions on graphs, where they were identified as the kernel of the Laplacian operator on graphs [40]. The graph Laplacian and its kernel are important tools in studying graph properties, see [48, 50] for surveys. Eckmann [28] introduced the higher-order Laplacian for simplicial complexes, and proved the isomorphism of harmonic chains and homology. Guglielmi et al. [33] studied the stability of higher-order Laplacians. Horak and Jost [38] defined a weighted Laplacian for simplicial complexes. Already their theoretical results on Laplacian [38] anticipated the possibility of applications, as the harmonic chains are thought to contain important geometric information. This has been validated by recent results that use curves of eigenvalues of Laplacians in a filtration in data analysis [18, 52]. The Laplacian was applied to improve the mapper algorithm [49], and for coarsening triangular meshes [39]. The persistent Laplacian [47] and its stability [44] is an active research area. Due to the close relation of harmonic chains and Laplacians, harmonic chains could find applications in areas that Laplacians have been used. Computing reasonable representative cycles for persistent homology is also an active area of research. Here, usually an optimality criterion is imposed on cycles in a homology class to obtain a unique representative. For a single homology class, a number of works [16, 23, 25, 51, 7, 13, 17, 23, 41] consider different criteria for optimality of cycles. Hardness of computing optimal representatives has been studied by [17, 11, 12, 13, 5, 32, 25]. For persistent homology, Dey et al. [25] studied the hardness of choosing optimal cycles for persistence bars. Furthermore, De Gregorio et al. [21] used harmonic cycles in a persistent homology setting to compute the persistence barcode. Lieutier [43] studied the harmonic chains in persistent homology classes, called persistent harmonic forms.

Relation to the work of Basu and Cox. The most relevant work to ours is the inspiring work of Basu and Cox [2]. Basu and Cox had a similar goal as ours, namely, to associate geometric information to each bar in order to obtain a more interpretable data feature. To that end, they introduced the notion

of *harmonic persistent barcode*, by associating a subspace of harmonic chains to each bar in the *ordinary* persistence barcode. When the multiplicity of the bar is 1, the subspace is 1-dimensional. This is the space of harmonic chains that are born at s and die entering t . In general, this is a quotient subspace of harmonic chains at time s . Using orthogonality they can represent this subquotient as a subspace of the harmonic cycles at time s . As a result, they successfully assign a canonical harmonic cycle to a bar in the ordinary persistence diagram. We note that, in general, a bar in the persistence barcode cannot be represented using a single harmonic chain that *remains harmonic during the lifetime of the bar*. The harmonic cycle associated to a bar using the Basu-Cox approach is the initial harmonic representative of the bar, that is, the harmonic cycle that represents the bar at its birth. Basu and Cox also used the *terminal harmonic cycle* in some of their arguments, thus showing that the choice is not entirely canonical. However, Basu and Cox proved significant properties of the initial cycles in terms of what they call *relative essential content*. The novelty of our result is that, in contrast to [2], we define a new barcode distinct from the ordinary persistence barcode, in which each bar has a harmonic cycle associated with it which is harmonic during the lifetime of the bar. Basu and Cox also proved stability for their harmonic persistent barcode, by considering subspaces as points of a Grassmannian manifold and measuring distances in the Grassmannian. Such a distance quantifies the angles between subspaces, whereas our notions of stability are stronger in the sense that they use the classical bottleneck distance analogous to the ordinary persistence homology. Gülen et al. [34] studied a method that permits the construction of stable persistence diagrams that are equipped with a canonical choice of representative cycles for filtrations over arbitrary finite posets. If the underlying poset is a finite subset of the real line, using persistent Laplacians, they obtained harmonic cycles connected (through a certain isomorphism) to those identified by Basu and Cox.

3 Background

In this section, we review the notion of harmonic chains and persistent homology. Homology and cohomology are defined with real coefficients \mathbb{R} (instead of \mathbb{Z}_2); see App. A for a review of homology and cohomology. Let K be a simplicial complex and p the homology dimension (or equivalently, homology degree). $C_p(K)$, $Z_p(K)$, and $H_p(K)$ denote the p -th chain group, cycle group, and homology group of K , whereas $C^p(K)$, $Z^p(K)$, and $H^p(K)$ denote the p -th cochain group, cocycle group, and cohomology group of K , respectively. Groups across all dimensions are denoted as $C_*(K)$, $C^*(K)$, etc. We use ∂ and δ to denote boundary and coboundary operators, respectively.

3.1 Harmonic Cycles

Based on the standard notions of homology and cohomology with \mathbb{R} coefficients (see App. A), we identify chains and cochains via duality, i.e., $C_p(K) = C^p(K) = \mathbb{R}^{n_p}$, where n_p is the number of p -simplices. Therefore, we can talk about coboundaries of cycles in $Z_p(K)$. We first introduce the notion of harmonic chains.

Definition 1. The p -th *harmonic chain group* of K , denoted $\mathbb{H}_p(K)$, is the group of p -cycles that are also p -cocycles. Equivalently, $\mathbb{H}_p(K) := Z_p(K) \cap Z^p(K)$. Each element in $\mathbb{H}_p(K)$ is called a *harmonic p -chain*. The harmonic chain group in all dimensions is the group $\mathbb{H}(K) := \bigoplus_p \mathbb{H}_p(K)$.

We sometimes use *harmonic cycles* in place of *harmonic chains* to emphasize the fact that harmonic chains are cycles.

Lemma 2 ([28]). $\mathbb{H}_p(K)$ is isomorphic to $H_p(K)$ and $H^p(K)$. Specifically, each homology and cohomology class has a unique harmonic cycle in it.

Harmonic cycles enjoy certain geometric properties. As an example, we mention the following proposition 3; see [22, Proposition 3] for a proof. In other words, a harmonic cycle is the chain with the least squared-norm in a cohomology class.

Proposition 3 ([22]). Let $\alpha \in C^p(K)$ be a cochain. There is a unique solution $\bar{\alpha}$ to the least-squares minimization problem $\arg \min_{\bar{\alpha}} \{ \|\bar{\alpha}\|^2 \mid \exists \gamma \in C^{p-1}(K); \alpha = \bar{\alpha} + \delta\gamma \}$. Moreover, $\bar{\alpha}$ is characterized by the relation $\partial\bar{\alpha} = 0$.

There is an alternative definition of harmonic cycles. Consider the natural inner product on $C_p(K)$ given by $\langle \sigma_i, \sigma_j \rangle = \delta_{i,j}$. The harmonic chain group can be defined as $\mathbb{H}_p(K) = Z_p(K) \cap B_p(K)^\perp$. With this definition, the isomorphism of lemma 2 is realized by a map that sends $z + B_p(K)$ to its projection to $B_p(K)^\perp$. In addition, the harmonic cycles satisfy $\mathbb{H}_p(K) = \ker(\partial_p) \cap \ker(\partial_{p+1}^\perp)$. For a short proof of the equivalence among the definitions of harmonic cycles above, see [2]. Importantly, our algorithm relies on the fact that harmonic cycles are cocycles whose boundaries are zero.

3.2 Ordinary Persistence

Ordinary persistent homology takes a *filtration* of a simplicial complex K as input. A *continuous* filtration F assigns to each $r \in \mathbb{R}$ a subcomplex $K_r \subseteq K$ such that $K_r \subseteq K_s$ for $r \leq s$. Since K is finite, there are finitely many $t_0, t_1, \dots, t_m \in \mathbb{R}$ where K_{t_i} changes. We then abuse the notations slightly by letting $K_i := K_{t_i}$ and have a *discrete* form of F ,

$$F : \emptyset = K_0 \hookrightarrow K_1 \hookrightarrow \dots \hookrightarrow K_{m-1} \hookrightarrow K_m = K, \quad (1)$$

where each $K_i \hookrightarrow K_{i+1}$ is an inclusion. Unless stated otherwise, we assume that F is *simplex-wise*, i.e., each two K_i and K_{i+1} differ by at most a single simplex. For simplicity of the exposition, complexes in F sometimes are subscripted by real-valued “timestamps” of the form K_{t_i} (e.g., in Sec. 6) or subscripted by integers of the form K_i (e.g., in Sec. 5), which should not cause any confusions. Applying homology functor to Eq. (1), we obtain a sequence of homology groups and connecting linear maps (homomorphisms), forming a *persistence module*:

$$\mathcal{M} : H_p(K_0) \rightarrow H_p(K_1) \rightarrow \dots \rightarrow H_p(K_{m-1}) \rightarrow H_p(K_m). \quad (2)$$

For $s \leq t$, let $f_p^{s,t} : H_p(K_s) \rightarrow H_p(K_t)$ denote the map induced on the p -th homology by inclusion. The image of the map, $f_p^{s,t}(H_p(K_s)) \subseteq H_p(K_t)$, is called the p -th (s,t) -*persistent homology group*, denoted $H_p^{s,t}$. The group $H_p^{s,t}$ consists of homology classes which exist in K_s and survive until K_t . The dimensions of these vector spaces are the *persistent Betti numbers*, denoted $\beta_p^{s,t}$. An *interval module*, denoted $I = I[b, d)$, is a persistence module of the form

$$0 \rightarrow \dots \rightarrow 0 \rightarrow \mathbb{R} \rightarrow \dots \rightarrow \mathbb{R} \rightarrow 0 \rightarrow \dots \rightarrow 0.$$

In the above, \mathbb{R} is generated by a homology class and the connecting homomorphisms map generator to generator. We have $I_r = \mathbb{R}$ for $b \leq r < d$ and $I_r = 0$ for other r . Any persistence module can be decomposed into a collection of interval modules in a unique way [45]. The collection of $[b, d)$ for all interval modules is called the *persistence barcode*. When plotted as points in an extended plane, the result is the equivalent *persistence diagram*.

Stability of Persistence Diagram/Barcode. The stability of persistence diagrams (or barcodes) is a crucial property for applications. It says that small changes in data lead to small changes in the persistence diagrams. We only review the stability for sublevel-set filtrations here; see Sec. 6.1 for more on stability of persistence modules. Let D and D' denote two persistence diagrams. Recall that a persistence diagram is a multi-set of points in the extended plane (each of which is a birth-death pair) which also contains all points on the diagonal. The *bottleneck distance* of D, D' is defined as

$$d_B(D, D') = \inf_\gamma \sup_{p \in D} \|p - \gamma(p)\|_\infty,$$

where γ ranges over all bijections between D and D' and $\|\cdot\|_\infty$ is the largest absolute value of differences of the points' coordinates.

A function $\tilde{f} : |K| \rightarrow \mathbb{R}$ is called *simplex-wise linear* if it is linear on each simplex. Let $K_r = \{\sigma \in K \mid \forall x \in |\sigma|, f(x) \leq r\}$ be the *sublevel set complex* at value $r \in \mathbb{R}$. The complexes K_r and the inclusions between them form a *sublevel set filtration* \tilde{F} (which is not necessarily simplex-wise). We denote the persistence diagram of \tilde{F} as $\text{Dgm}(\tilde{f})$. We refer to [19, 14] for proof of the following Theorem 29. See [19, 14] for the stability of ordinary persistence.

Theorem 4. Let $\tilde{f}, \tilde{g} : |K| \rightarrow \mathbb{R}$ be simplex-wise linear functions. Then

$$d_B(\text{Dgm}(\tilde{f}), \text{Dgm}(\tilde{g})) \leq \|\tilde{f} - \tilde{g}\|_\infty.$$

3.3 Zigzag Persistence

We provide a brief overview of zigzag persistence; see [8, 9] for details. A zigzag module

$$\mathcal{M} : V_0 \xleftarrow{g_0} V_1 \xleftarrow{g_1} \dots \xleftarrow{g_{k-1}} V_k$$

is a sequence of vector spaces connected by linear maps which could be forward or backward, i.e., each g_i could be $g_i : V_i \rightarrow V_{i+1}$ or $g_i : V_i \leftarrow V_{i+1}$. The module \mathcal{M} decomposes into a direct sum of interval modules $I[b, d]$ of the form

$$0 \longleftrightarrow \dots \longleftrightarrow 0 \longleftrightarrow \mathbb{R} \longleftrightarrow \dots \longleftrightarrow \mathbb{R} \longleftrightarrow 0 \dots \longleftrightarrow 0$$

with 1-dimensional vector spaces in the range $[b, d]$. The multi-set of intervals in the decomposition defines the *barcode* of \mathcal{M} , denoted as $B(\mathcal{M})$.

Conventions. In this paper, we may omit the subscript/dimension of a homology group if there is no danger of ambiguity. Moreover, we use the terms persistence barcode and persistence diagram interchangeably.

4 Harmonic Chain Barcodes and Representatives

As reviewed in Sec. 3.2, by directly taking the homology functor, an increasing filtration of simplicial complexes leads to an *ordinary persistence module* consisting of homology groups [15, 27]. These homology groups are connected by forward maps of the form $H(K_i) \rightarrow H(K_{i+1})$. The ordinary persistence module then decomposes into interval modules, which define the *ordinary persistence barcode*. In this section, we show that the harmonic chain groups of all the complexes in a filtration constitute an abstract *zigzag persistence module* (see Sec. 3.3). The main idea is that we take the harmonic chain groups along the filtration, where the groups could grow or shrink, resulting in a zigzag module. Moreover, the maps in this zigzag module are inclusions. Like any zigzag module [8], the module of harmonic chain groups decomposes into interval modules. These intervals form the harmonic chain barcode, the main object of interest in this paper.

Throughout the section, consider a simplex-wise filtration

$$F : \emptyset = K_0 \xrightarrow{\sigma_0} K_1 \xrightarrow{\sigma_1} \dots \xrightarrow{\sigma_{m-1}} K_m = K,$$

where each K_{i+1} differs from K_i by the addition of a simplex σ_i . Recall that $K_i := K_{t_i}$ for $t_i \in \mathbb{R}$ where K_{t_i} is a complex from a *continuous* filtration indexed over \mathbb{R} ; see Sec. 3.2.

Proposition 5. For each inclusion $K_i \xrightarrow{\sigma_i} K_{i+1}$ in F :

$$\dim(\mathbb{H}(K_{i+1})) = \dim(\mathbb{H}(K_i)) \pm 1.$$

Proof. This follows from Lemma 2 and some well-known facts in persistence (see [27, 29]). \square

Definition 6. A simplex σ_i inserted in F is called *positive* if $\dim(\mathbb{H}(K_{i+1})) = \dim(\mathbb{H}(K_i)) + 1$, and *negative* if $\dim(\mathbb{H}(K_{i+1})) = \dim(\mathbb{H}(K_i)) - 1$.

We describe how we connect the harmonic chain groups of complexes in F by inclusions. For each K_i and each chain $c = \sum_{j=0}^{i-1} \alpha_j \sigma_j$ in $C_p(K_i)$, we identify c as a chain $c = \sum_{j=0}^{m-1} \alpha_j \sigma_j$ in $C_p(K)$, where $\alpha_j = 0$ for $j \geq i$. This makes both $C_p(K_i)$ and $C_p(K_{i+1})$ a subspace of $C_p(K)$. We then have the following inclusion:

$$Z_p(K_i) \hookrightarrow Z_p(K_{i+1}). \quad (3)$$

Recall that $\mathbb{H}_p(K_i) := Z_p(K_i) \cap Z^p(K_i)$, which means that $\mathbb{H}_p(K_i) \subseteq Z_p(K_i) \subseteq C_p(K)$. Hence, we also identify each harmonic cycle in $\mathbb{H}_p(K_i)$ as a chain in $C_p(K)$. We then observe in theorem 7 a similar inclusion as in Eq. (3) between any harmonic chain groups $\mathbb{H}_p(K_i)$ and $\mathbb{H}_p(K_{i+1})$, with a possible flip on the direction.

Theorem 7. For each arrow $K_i \xrightarrow{\sigma_i} K_{i+1}$ in F , where σ_i is a p -simplex:

- There is an inclusion $\mathbb{H}_p(K_i) \hookrightarrow \mathbb{H}_p(K_{i+1})$ if σ_i is positive;
- And there is an inclusion $\mathbb{H}_{p-1}(K_i) \hookrightarrow \mathbb{H}_{p-1}(K_{i+1})$ if σ_i is negative.

In addition, in each case the harmonic chain groups in other dimensions remain unchanged, i.e., $\mathbb{H}_q(K_i) = \mathbb{H}_q(K_{i+1})$ for any other $q \notin \{p, p-1\}$.

Proof. The only harmonic chain groups that might change from K_i to K_{i+1} are those in dimension p because cycle and cocycle groups in other dimensions do not change.

First consider Case I that σ_i is positive. Let $\iota : K_i \hookrightarrow K_{i+1}$ be the inclusion map. As noted above, we identify any $c \in C_*(K_i) = C^*(K_i)$ with $\iota_\#(c) \in C_*(K_{i+1}) = C^*(K_{i+1})$.

Case I.1: $\mathbb{H}_p(K_i) \subseteq \mathbb{H}_p(K_{i+1})$. Take $z \in \mathbb{H}_p(K_i)$. Obviously, $\iota_\#(z)$ is a cycle in K_{i+1} . Moreover, for any $c \in C_{p+1}(K_{i+1})$, $\delta(\iota_\#(z))(c) = \iota_\#(z)(\partial c)$. Since $C_{p+1}(K_i) = C_{p+1}(K_{i+1})$, c and hence ∂c exist in K_i , meaning that $\iota_\#(z)(\partial c) = z(\partial c) = (\delta z)(c) = 0$. It follows that $\iota_\#(z)$ is a cocycle in K_{i+1} . Therefore, $\mathbb{H}_p(K_i) \subseteq \mathbb{H}_p(K_{i+1})$.

Case I.2: $\mathbb{H}_{p-1}(K_i) = \mathbb{H}_{p-1}(K_{i+1})$. Take $z \in \mathbb{H}_{p-1}(K_{i+1})$. Since σ_i is a positive p -simplex, we have $Z_{p-1}(K_{i+1}) = Z_{p-1}(K_i)$ and $B_{p-1}(K_i) = B_{p-1}(K_{i+1})$. So $z \in Z_{p-1}(K_i)$ and we consider z as a cochain in K_i . Then, for any $c \in C_p(K_i)$, $\delta(z)(c) = z(\partial c) = 0$, with the last equality due to $\partial c \in B_{p-1}(K_i) = B_{p-1}(K_{i+1})$. Therefore, $\mathbb{H}_p(K_{i+1}) \subseteq \mathbb{H}_p(K_i)$. Take $z \in \mathbb{H}_{p-1}(K_i)$. For any $c \in C_p(K_{i+1})$, $\delta(\iota_\#z)(c) = \iota_\#z(\partial c) = 0$, with the last equality due to $\partial c \in B_{p-1}(K_{i+1}) = B_{p-1}(K_i)$. Therefore, $\mathbb{H}_{p-1}(K_i) = \mathbb{H}_{p-1}(K_{i+1})$.

Now consider Case II that σ_i is negative.

Case II.1: $\mathbb{H}_p(K_{i+1}) = \mathbb{H}_p(K_i)$. Since σ_i is negative, $Z_p(K_{i+1}) = Z_p(K_i)$ and $B_p(K_{i+1}) = B_p(K_i)$. The verification for this case is then the same as the verification for Case I.2 with a shift on the homology degree.

Case II.2: $\mathbb{H}_{p-1}(K_{i+1}) \subseteq \mathbb{H}_{p-1}(K_i)$. Take $z \in \mathbb{H}_{p-1}(K_{i+1})$. We have $Z_{p-1}(K_{i+1}) = Z_{p-1}(K_i)$. Therefore, $z \in Z_{p-1}(K_i)$ and we consider z as a cochain in K_i . For any $c \in C_p(K_i)$, $\delta(z)(c) = z(\partial c) = 0$, with the last equality due to $\partial c \in B_{p-1}(K_i) \subseteq B_{p-1}(K_{i+1})$. Therefore, $\mathbb{H}_{p-1}(K_{i+1}) \subseteq \mathbb{H}_{p-1}(K_i)$. \square

Definition 8 (Harmonic chain barcode). Consider the following *harmonic zigzag module*

$$\mathbb{H}(F) : \mathbb{H}(K_0) \leftrightarrow \mathbb{H}(K_1) \leftrightarrow \cdots \leftrightarrow \mathbb{H}(K_m), \quad (4)$$

where the harmonic chain groups are connected by either forward inclusions (e.g., $\mathbb{H}(K_i) \rightarrow \mathbb{H}(K_{i+1})$) or backward inclusions (e.g., $\mathbb{H}(K_i) \leftarrow \mathbb{H}(K_{i+1})$); see Theorem 7. Define the *harmonic chain barcode* $\mathbb{B}^{\mathbb{H}}(F)$ of F as the barcode of the zigzag module $\mathbb{H}(F)$, that is,

$$\mathbb{B}^{\mathbb{H}}(F) := \mathbb{B}(\mathbb{H}(F)).$$

In general, the harmonic chain barcode is different from the ordinary persistence barcode for a filtration; see Fig. 2. In this paper, we also consider the zigzag module $\mathbb{H}_p(F)$ derived by taking $\mathbb{H}_p(K_i)$ on each K_i in F . While the p -th harmonic chain groups in $\mathbb{H}_p(F)$ are still connected by forward or backward inclusions, we may have $\mathbb{H}_p(K_i) = \mathbb{H}_p(K_{i+1})$ for two consecutive groups in $\mathbb{H}_p(F)$. We therefore define the p -th *harmonic chain barcode* $\mathbb{B}_p^{\mathbb{H}}(F)$ of F as the barcode of $\mathbb{H}_p(F)$, i.e., $\mathbb{B}_p^{\mathbb{H}}(F) := \mathbb{B}(\mathbb{H}_p(F))$. Since $\mathbb{H}(F) = \bigoplus_p \mathbb{H}_p(F)$ (following from Theorem 7), we have $\mathbb{B}^{\mathbb{H}}(F) = \bigsqcup_p \mathbb{B}_p^{\mathbb{H}}(F)$.

Harmonic Representatives. In the rest of the section, we define harmonic representatives.

Proposition 9. Let $[b, d]$ be an interval in $\mathbb{B}^{\mathbb{H}}(F)$. The inclusion $\mathbb{H}(K_{b-1}) \hookrightarrow \mathbb{H}(K_b)$ in $\mathbb{H}(F)$ is forward. Moreover, if $d < m$, then the inclusion $\mathbb{H}(K_d) \leftarrow \mathbb{H}(K_{d+1})$ is backward.

Proof. This follows from Theorem 7 and the fact that $\dim(\mathbb{H}(K_b)) = \dim(\mathbb{H}(K_{b-1})) + 1$ and $\dim(\mathbb{H}(K_{d+1})) = \dim(\mathbb{H}(K_d)) - 1$. \square

Representatives for general zigzag modules were introduced in [4, 46] (see also [26]), which consist of a sequence of cycles for each interval. However, since the harmonic chain groups are connected by inclusion maps in $\mathbb{H}(F)$, we have:

Proposition 10. Each representative for an interval in $\mathbb{B}^{\mathbb{H}}(F)$ contains a single harmonic cycle.

We then adapt the definition of representatives for general zigzag modules [26, 46] and define harmonic representatives as follows:

Definition 11 (Harmonic representative). A *harmonic p -representative* (or simply *p -representative*) for an interval $[b, d] \in \mathbb{B}_p^{\mathbb{H}}(F)$ is a p -cycle $z \in \mathbb{H}_p(K_i)$ for $i \in [b, d]$ satisfying:

Birth condition: z is born in $\mathbb{H}_p(K_b)$, i.e., $z \in \mathbb{H}_p(K_b) \setminus \mathbb{H}_p(K_{b-1})$ (notice that $b > 0$);

Death condition: z dies leaving $\mathbb{H}_p(K_d)$, i.e., $z \in \mathbb{H}_p(K_d) \setminus \mathbb{H}_p(K_{d+1})$ if $d < m$.

Sometimes we relax the restriction of $[b, d] \in \mathbb{B}_p^{\mathbb{H}}(F)$ and have a harmonic representative for an arbitrary integer interval $[b, d] \subseteq [0, m]$. App. B details the original definition of zigzag representatives and justifies Proposition 10 and Definition 11.

5 A Cubic-Time Algorithm for Computing Harmonic Chain Barcodes

In this section, we propose an $O(m^3)$ algorithm for computing the harmonic chain barcode and its harmonic representatives given a filtration containing m insertions. We first overview the algorithm and then describe the implementation. While there have been algorithms [9, 26, 46] for computing zigzag barcodes in the general case, these algorithms target zigzag modules induced from directly *taking the homology functor on zigzag filtrations*. In contrast, our algorithm targets the special type of zigzag module $\mathbb{H}(F)$, where harmonic chain groups are derived from an *ordinary non-zigzag* filtration and are connected by inclusions.

For simplicity, when describing the algorithm, complexes in a filtration are always indexed by integers instead of the real-valued timestamps (see Sec. 3.2). Again, we assume that the input is a simplex-wise filtration $F : \emptyset = K_0 \xrightarrow{\sigma_0} K_1 \xrightarrow{\sigma_1} \dots \xrightarrow{\sigma_{m-1}} K_m = K$, where each K_{i+1} differs from K_i by the addition of a simplex σ_i .

Algorithm 1 provides an overview: our algorithm computes the harmonic chain barcode by iteratively maintaining the harmonic representatives. It processes the insertions in F one by one and finds *pairings* of the *birth indices* (starting points of the intervals) and *death indices* (ending points of the intervals) to form intervals in $\mathbb{B}^{\mathbb{H}}(F)$. When we encounter a new birth index, it is initially *unpaired*; when we encounter a new death index, an unpaired birth index is chosen to pair with the death index.

The following definition helps present the algorithm.

Definition 12. For an interval $[b, i] \subseteq [0, m]$, a *partial p -representative* for $[b, i]$ is a p -representative as in Definition 11 by ignoring the death condition.

Algorithm 1. Let U^p be the set of unpaired birth indices for each homology degree p , where $U^p = \emptyset$ initially. Before each iteration that processes the insertion $K_i \xrightarrow{\sigma_i} K_{i+1}$, we maintain a p -cycle z for each $b \in U^p$ that is a partial representative for the interval $[b, i]$. We use partial representatives to determine a finalized representative when a birth index is paired with a death index (by making sure the death condition is satisfied).

When processing the insertion of a p -simplex σ_i via $K_i \xrightarrow{\sigma_i} K_{i+1}$, we proceed as follows:

If σ_i is positive:

- Since $\dim(\mathbb{H}_p(K_{i+1})) = \dim(\mathbb{H}_p(K_i)) + 1$ (by Theorem 7), we add a new birth index $i + 1$ to U^p .
- Find a harmonic p -cycle $z \in \mathbb{H}_p(K_{i+1}) \setminus \mathbb{H}_p(K_i)$, and let z be the partial representative for $i + 1 \in U^p$.

If σ_i is negative:

- Since $\dim(\mathbb{H}_{p-1}(K_{i+1})) = \dim(\mathbb{H}_{p-1}(K_i)) - 1$, we have a new death index i .
- Let $U^{p-1} = \{b_j \mid j = 1, \dots, k\}$, where each b_j has a partial $(p-1)$ -representative z_j .
- Let $U' = \{b_j \in U^{p-1} \mid z_j \notin \mathbb{H}_{p-1}(K_{i+1})\}$, i.e., U' contains all birth indices in U^{p-1} whose partial representatives do not persist to K_{i+1} .
- Pair the *smallest* (i.e., the “oldest”) index $b_{j^*} \in U'$ with i which forms a new interval $[b_{j^*}, i] \in \mathbb{B}_{p-1}^{\mathbb{H}}(F)$. Assign z_{j^*} as the representative for $[b_{j^*}, i] \in \mathbb{B}_{p-1}^{\mathbb{H}}(F)$ and remove i from U^{p-1} .
- Consider each $b_j \in U' \setminus \{b_{j^*}\}$. We have that $z_j \notin \mathbb{H}_{p-1}(K_{i+1})$ because $\delta(z_j)$ becomes non-zero in K_{i+1} (∂z_j is always zero after being born). Also, the only reason that $\delta(z_j) \neq 0$ in K_{i+1} is because $\alpha_j := \delta(z_j)(\sigma_i) = z_j(\partial\sigma_i) \neq 0$. Let $\alpha_* = z_{j^*}(\partial\sigma_i)$. Update the partial representative for b_j as $z_j := z_j - (\alpha_j/\alpha_*) \cdot z_{j^*}$ so that z_j now persists to $\mathbb{H}_{p-1}(K_{i+1})$.

After processing all the insertions, for each b in each U^p with a partial representative z , let $[b, m]$ form an interval in $\mathbb{H}_p(F)$ with a representative z .

Example. Fig. 1 provides an example of how Algorithm 1 computes harmonic chain barcode $\mathbb{H}_1(F)$ and representatives for a filtration F , with the resulting barcode in Fig. 2. For simplicity, K_0, K_1, K_2 are omitted and vertex insertions are ignored. In K_4, K_5 , and K_7 , new 1-cycles are born which are also harmonic cycles due to a lack of triangles. The partial representatives z_4, z_5, z_7 for the indices $U^1 = \{4, 5, 7\}$ all persist till K_7 . When the triangle abe is inserted in K_8 (producing a death index 7), $\delta(z_4)(abe) = 1$, $\delta(z_5)(abe) = 1$, and $\delta(z_7)(abe) = 3$. We pair 4 $\in U^1$ with 7 and have $[4, 7] \in \mathbb{H}_1(F)$ with a representative z_4 . We also let $z_5 := z_5 - z_4$ and $z_7 := z_7 - 3z_4$, which now both persist to $\mathbb{H}_1(K_8)$. The remaining steps are similar. Notice that when abe is inserted, the “alive” bar represented by the boundary of abe (i.e., $ab + be - ae$) is not killed. This is a significant difference from ordinary persistence (which will kill the alive bar represented by $\partial(abe)$ when abe is inserted).

Remark 13. Algorithm 1 chooses the “oldest” birth, among the options, to pair with a death while the ordinary persistence chooses the “youngest” one [29]. A brief explanation is that a summation of representatives *persists* to the next harmonic chain group in $\mathbb{H}(F)$, whereas a summation of representatives in the ordinary persistence *becomes trivial* in the next homology group (and cannot persist). We refer to [26, 46] for a formal definition of the different types of birth/death ends and how they impact the computation of persistence.

The following (rephrased) proposition from [24] helps prove the correctness of Algorithm 1:

Proposition 14 (Proposition 9, [24]). If a pairing π of the birth and death indices in $\mathbb{H}(F)$ satisfies that each interval from π has a harmonic representative, then π induces the harmonic chain barcode $\mathbb{B}^{\mathbb{H}}(F)$.

Theorem 15. Algorithm 1 correctly computes the harmonic chain barcode for filtration F .

Proof. We first show by induction that before Algorithm 1 processes each σ_i , the p -cycle z maintained for any $b \in U^p$ is a partial p -representative for $[b, i]$. Suppose that the claim is true before processing σ_i . If σ_i is positive, index $i+1$ is added to U^p and we assign $z \in \mathbb{H}_p(K_{i+1}) \setminus \mathbb{H}_p(K_i)$ to $i+1$, which is clearly a partial representative for $[i+1, i+1]$. For an index b previously in U^p having a partial representative z , since $\mathbb{H}_p(K_i) \subseteq \mathbb{H}_p(K_{i+1})$ (Theorem 7), we have that z is still a partial representative for the interval $[b, i+1]$.

In the case that σ_i is negative, whenever we update a representative z_j as $z_j - (\alpha_j/\alpha_*) \cdot z_{j^*}$, we have that $b_{j^*} < b_j$ and hence the updated z_j remains born in $\mathbb{H}_{p-1}(K_{b_j})$. Therefore, the new z_j is still a partial representative for $[b, i]$, which is also a partial representative for $[b, i+1]$ because now $z_j \in \mathbb{H}_{p-1}(K_{i+1})$.

By Proposition 14, we only need to show that each interval output by the algorithm admits a harmonic representative. This follows from the algorithm. For example, whenever we output an interval $[b_{j^*}, i] \in \mathbb{B}_{p-1}^{\mathbb{H}}(F)$ when σ_i is negative, we have $z_{j^*} \notin \mathbb{B}_{p-1}^{\mathbb{H}}(K_{i+1})$, which ensures the death condition. \square

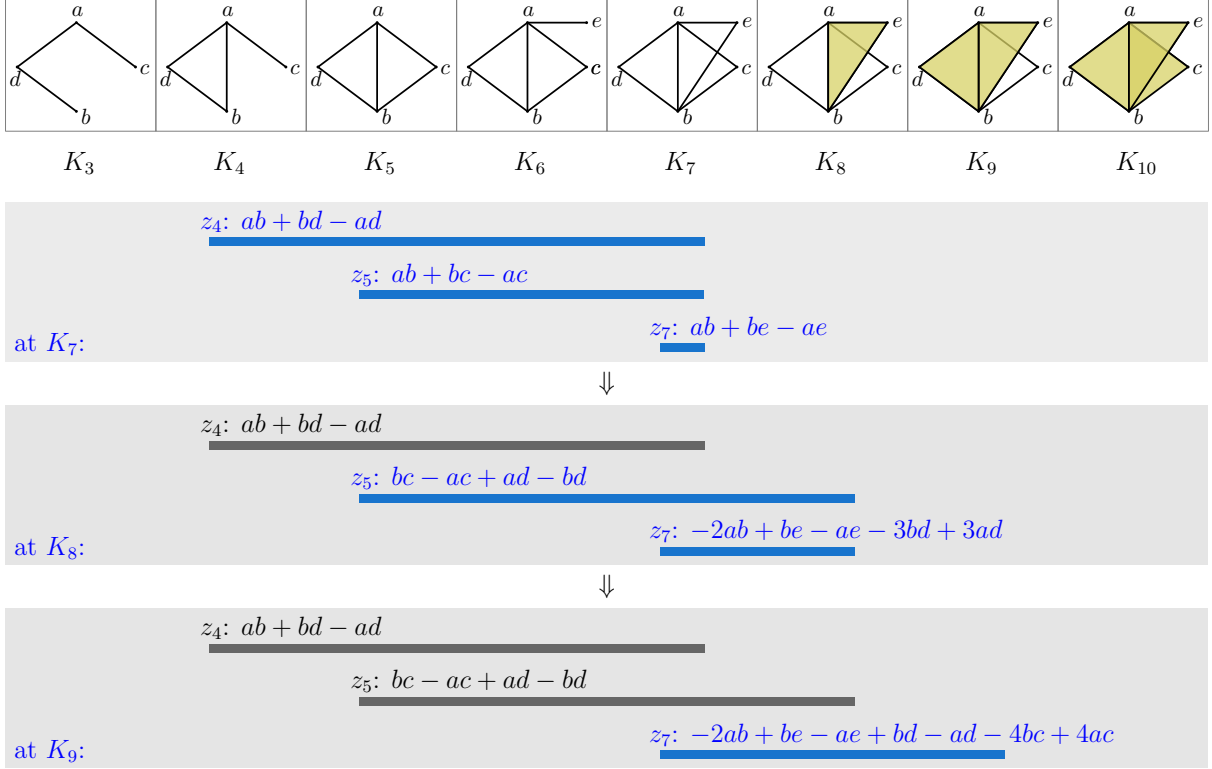


Figure 1: An example of the computation of harmonic chain barcode $\mathbb{H}_1(F)$ and representatives.

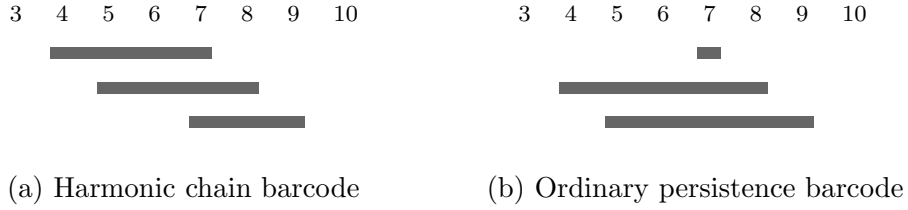


Figure 2: Harmonic chain barcode and ordinary persistence barcode for the filtration in Fig. 1. Deviating from conventions in ordinary persistence, bars are drawn as closed integer intervals, e.g., $[7, 7]$ in the ordinary barcode is killed by the addition of abe in K_8 .

5.1 Implementation

Before detailing the implementation, we first have the following fact:

Proposition 16. When a p -simplex σ_i is added from K_i to K_{i+1} , one has:

- If σ_i is positive, then

$$\dim(Z^p(K_{i+1})) = \dim(Z^p(K_i)) + 1 \text{ and} \\ \dim(B^p(K_{i+1})) = \dim(B^p(K_i)).$$

- If σ_i is negative, then

$$\dim(Z^p(K_{i+1})) = \dim(Z^p(K_i)) + 1, \\ \dim(B^p(K_{i+1})) = \dim(B^p(K_i)) + 1, \text{ and} \\ \dim(Z^{p-1}(K_{i+1})) = \dim(Z^{p-1}(K_i)) - 1.$$

Furthermore, in each case, all other cocycle or coboundary groups not mentioned above stay the same from K_i to K_{i+1} .

Proof. We first show that $\dim(Z^p(K_{i+1})) = \dim(Z^p(K_i)) + 1$ whether σ_i is positive or negative. Let

$$\iota^\sharp : C^p(K_{i+1}) \rightarrow C^p(K_i)$$

be the cochain map induced by inclusion. Clearly, we have $\iota^\sharp(Z^p(K_{i+1})) \subseteq Z^p(K_i)$ [36]. Let

$$j^\sharp : Z^p(K_{i+1}) \rightarrow Z^p(K_i)$$

be the restriction of ι^\sharp . We show that j^\sharp is surjective and the kernel of j^\sharp is 1-dimensional. First, for any cocycle $\phi \in Z^p(K_i)$, we define a cocycle $\phi' \in Z^p(K_{i+1})$ where $\phi'(\sigma_i) = 0$ and values of ϕ' on other p -simplices are the same as ϕ . We have that $j^\sharp(\phi') = \phi$ and so j^\sharp is surjective. Moreover, let $\hat{\sigma}_i \in Z^p(K_{i+1})$ be the dual of σ_i . We have that $\hat{\sigma}_i$ generates the kernel of j^\sharp .

We also notice that the coboundary maps

$$\delta^{p-2} : C^{p-2}(K_i) \rightarrow C^{p-1}(K_i)$$

and

$$\delta^{p-2} : C^{p-2}(K_{i+1}) \rightarrow C^{p-1}(K_{i+1})$$

are the same, and so $B^{p-1}(K_{i+1}) = B^{p-1}(K_i)$.

Suppose that σ_i is positive. We have $\dim(H^p(K_{i+1})) = \dim(H^p(K_i)) + 1$. Since

$$\begin{aligned} \dim(H^p(K_i)) &= \dim(Z^p(K_i)) - \dim(B^p(K_i)), \\ \dim(H^p(K_{i+1})) &= \dim(Z^p(K_{i+1})) - \dim(B^p(K_{i+1})), \text{ and} \\ \dim(Z^p(K_{i+1})) &= \dim(Z^p(K_i)) + 1, \end{aligned}$$

we have $\dim(B^p(K_{i+1})) = \dim(B^p(K_i))$. Similarly, since

$$\begin{aligned} H^{p-1}(K_{i+1}) &\approx H^{p-1}(K_i), \\ B^{p-1}(K_{i+1}) &= B^{p-1}(K_i), \text{ and} \\ C^{p-1}(K_{i+1}) &= C^{p-1}(K_i), \end{aligned}$$

we have $Z^{p-1}(K_{i+1}) = Z^{p-1}(K_i)$.

When σ_i is negative, the statements regarding the dimensions of the cocycle and coboundary groups in the proposition can be similarly obtained.

To see that other cocycle or coboundary groups do not change, we provide arguments for the groups in degree $p+1$ and the justification for groups in other degrees is omitted. We first have $Z^{p+1}(K_{i+1}) = Z^{p+1}(K_i)$ because the two maps $\delta^{p+1} : C^{p+1}(K_i) \rightarrow C^{p+2}(K_i)$ and $\delta^{p+1} : C^{p+1}(K_{i+1}) \rightarrow C^{p+2}(K_{i+1})$ are the same. Moreover, we have $B^{p+1}(K_{i+1}) = B^{p+1}(K_i)$ because σ_i has no cofaces in K_{i+1} . \square

Pseudo-cochains. We introduce the notion of pseudo-cochains which are more ‘‘concise’’ versions of cochains. These pseudo-cochains help maintain a coboundary basis in our implementation. Proofs of Propositions 17, 19 and 21 follow directly from definitions and are omitted. Proposition 17 says that the coboundary of a p -cochain ϕ is completely determined by how ϕ maps the p -boundaries to real values:

Proposition 17. Let $\phi : C_p(K_i) \rightarrow \mathbb{R}$ and $\psi : C_p(K_i) \rightarrow \mathbb{R}$ be two p -cochains of K_i . Also, let $\bar{\phi} : B_p(K_i) \rightarrow \mathbb{R}$ and $\bar{\psi} : B_p(K_i) \rightarrow \mathbb{R}$ be restriction of ϕ and ψ to $B_p(K_i)$ respectively. One has that $\delta(\phi) = \delta(\psi)$ if and only if $\bar{\phi} = \bar{\psi}$.

Definition 18. Define a p -pseudo-cochain ψ in K_i as a map $\psi : B_p(K_i) \rightarrow \mathbb{R}$. Define the *coboundary* of ψ as the $(p+1)$ -cochain $\psi \circ \bar{\partial}$, where $\bar{\partial} : C_{p+1}(K_i) \rightarrow B_p(K_i)$ is the restriction of ∂ to its image. We abuse the notation slightly and denote the coboundary of ψ as $\delta(\psi)$.

Proposition 19 says that coboundaries of a complex are completely determined by the pseudo-cochains:

Proposition 19. The space of coboundaries of all p -pseudo-cochains of K_i equals $B^{p+1}(K_i)$.

Definition 20. Given a basis $\mathcal{R} = \{\zeta_1, \dots, \zeta_r\}$ of $B_p(K_i)$ and a column vector $\vec{v} = (\alpha_1, \dots, \alpha_r)^T$, we say that \vec{v} encodes the p -pseudo-cochain $\psi : B_p(K_i) \rightarrow \mathbb{R}$ w.r.t the basis \mathcal{R} if $\psi(\zeta_j) = \alpha_j$ for each j .

Proposition 21 says that summations and scalar multiplications on the column vectors encoding p -pseudo-cochains commute with the coboundary operator:

Proposition 21. Fix a basis $\mathcal{R} = \{\zeta_1, \dots, \zeta_r\}$ of $B_p(K_i)$. Let \vec{u}, \vec{v} be two column vectors encoding p -pseudo-cochains ψ, ψ' w.r.t \mathcal{R} respectively. For an $\alpha \in \mathbb{R}$, one has that $\vec{u} + \alpha\vec{v}$ encodes the p -pseudo-cochains $\psi + \alpha \cdot \psi'$ w.r.t \mathcal{R} and $\delta(\psi + \alpha \cdot \psi') = \delta(\psi) + \alpha \cdot \delta(\psi')$.

In this paper, when a basis \mathcal{R} of $B_p(K_i)$ is clear, we abuse the notations and let $\delta(\vec{v}) := \delta(\psi)$, where \vec{v} is a vector encoding a p -pseudo-cochain ψ w.r.t \mathcal{R} .

Representation of chains and cochains. We represent chains as matrix columns and make no distinction between a column vector and the chain it represents. Specifically, with $C_*(K_i) \subseteq C_*(K)$ and a natural basis $\{\sigma_0, \sigma_1, \dots, \sigma_{m-1}\}$ for $C_*(K)$, each chain

$$c = \sum_{k=0}^{i-1} \alpha_k \sigma_k \in C_*(K_i)$$

is represented as a column vector

$$(\alpha_0, \alpha_1, \dots, \alpha_{m-1})^T,$$

where $\alpha_k = 0$ for each $k \geq i$. For a matrix M , we denote its j -th column as $M[j]$. For a chain z as a column vector, we denote its k -th entry as $z[k]$. Hence, the entry in the k -th row and j -th column in M is denoted as $M[j][k]$. Moreover, we let the *pivot* of $M[j]$ be the index of the lowest non-zero entry in $M[j]$ which is denoted as $\text{pivot}(M[j])$.

Cochains are similarly represented as matrix columns by taking the dual basis

$$\{\hat{\sigma}_0, \hat{\sigma}_1, \dots, \hat{\sigma}_{m-1}\}$$

for $C^*(K)$. Notice that since chains and cochains are identified, a matrix column

$$(\alpha_0, \alpha_1, \dots, \alpha_{m-1})^T$$

can represent *both* the chain $\sum_{k=0}^{m-1} \alpha_k \sigma_k$ and the cochain $\sum_{k=0}^{m-1} \alpha_k \hat{\sigma}_k$. Moreover, due to the identification, a formal sum

$$\sum_{k=0}^{m-1} \alpha_k \hat{\sigma}_k$$

can also denote a chain, which should not cause any confusions.

Matrices maintained. The only step in Algorithm 1 that cannot be easily implemented is finding a new harmonic cycle born in $\mathbb{H}_p(K_{i+1})$ when σ_i is positive. We can do this naively by computing a basis for the kernel of δ in K_{i+1} , and check all cocycles in the basis to see if they are independent of the existing set of harmonic representatives maintained for K_i . This, however, requires at least $\Theta(m^3)$ per simplex insertion.

For a more efficient implementation, before iteration i which processes the insertion $K_i \xrightarrow{\sigma_i} K_{i+1}$, we maintain the following matrices for each homology degree p :

1. \mathbb{H}^p : Columns in \mathbb{H}^p are partial p -representatives for all indices in U^p , which form a *harmonic cycle basis* for $\mathbb{H}_p(K_i)$; see App. C for justification.
2. \mathbb{R}^p : Columns in \mathbb{R}^p form a *boundary basis* with distinct pivots for $B_p(K_i)$. Notice that \mathbb{R}^p is indeed the “reduced” matrix in the ordinary persistence algorithm [20] with only p -chains and without zero columns.
3. Cob^p : Columns in Cob^p form a *coboundary basis* for $B^p(K_i)$.

4. \mathbf{SC}^p : Columns in \mathbf{SC}^p encode p -pseudo-cochains in K_i w.r.t the basis \mathbf{R}^p whose coboundaries are columns in \mathbf{Cob}^{p+1} . More specifically, $\mathbf{SC}^p, \mathbf{Cob}^{p+1}$ have the same number of columns and for each j , $\mathbf{Cob}^{p+1}[j] = \delta(\psi_j)$ where ψ_j is the p -pseudo-cochain encoded by $\mathbf{SC}^p[j]$ w.r.t \mathbf{R}^p .
5. \mathbf{BoC}^p : Columns in \mathbf{BoC}^p are boundaries of the coboundaries in \mathbf{Cob}^{p+1} , i.e., $\mathbf{BoC}^p, \mathbf{Cob}^{p+1}$ have the same number of columns and $\mathbf{BoC}^p[j] = \partial(\mathbf{Cob}^{p+1}[j])$ for each j . We further ensure that columns in \mathbf{BoC}^p have distinct pivots so that the reduction process in Algorithm 3 can be done in $O(m^2)$ time.

In summary, columns in $\mathbf{SC}^{p-1}, \mathbf{Cob}^p$, and \mathbf{BoC}^{p-1} have one-to-one correspondence as follows:

$$\mathbf{SC}^{p-1}[j] \xrightarrow{\delta} \mathbf{Cob}^p[j] \xrightarrow{\partial} \mathbf{BoC}^{p-1}[j].$$

Other than \mathbf{H}^p which is already in Algorithm 1, the rationale for maintaining the matrices is as follows (assuming σ_i is a p -simplex):

- We use \mathbf{BoC}^{p-1} to find a linear combination ϕ of $\hat{\sigma}_i$ and cocycles in \mathbf{Cob}^p such that $\partial\phi = 0$ (see Algorithm 3). The cocycle ϕ is then a new harmonic p -cycle when σ_i is positive.
- \mathbf{SC}^{p-1} helps maintain the coboundary basis in \mathbf{Cob}^p .
- \mathbf{R}^{p-1} provides the boundary basis on which pseudo-cochains in \mathbf{SC}^{p-1} can be defined.

Initial reduction. When processing the insertion of a p -simplex σ_i , we first apply the reduction in Algorithm 2 on \mathbf{R}^{p-1} (which is indeed performed in the ordinary persistence algorithm [29]). The following Proposition 22 is well-known [27, 29]:

Proposition 22. If Algorithm 2 ends with $z = 0$, then σ_i is positive; otherwise, σ_i is negative.

Notice that besides determining whether σ_i is positive or negative, Algorithm 2 also ensures that \mathbf{R}^{p-1} represents a basis for $B_{p-1}(K_{i+1})$ in the next iteration (details discussed later).

Algorithm 2 Reduction based on \mathbf{R}^{p-1} for determining whether σ_i is positive or negative

- 1: $z \leftarrow \partial(\sigma_i)$
 - 2: **while** $z \neq 0$ and $\exists j$ s.t. $\text{pivot}(\mathbf{R}^{p-1}[j]) = \text{pivot}(z)$ **do**
 - 3: $k \leftarrow \text{pivot}(z)$
 - 4: $\alpha_1 \leftarrow z[k]$
 - 5: $\alpha_2 \leftarrow \mathbf{R}^{p-1}[j][k]$
 - 6: $z \leftarrow z - (\alpha_1/\alpha_2) \cdot \mathbf{R}^{p-1}[j]$
-

σ_i **is positive.** We need to find a new harmonic p -cycle born in K_{i+1} . For this, we perform another reduction on \mathbf{BoC}^{p-1} and \mathbf{Cob}^p in Algorithm 3.

Algorithm 3 Reduction based on $\mathbf{BoC}^{p-1}, \mathbf{Cob}^p$ for finding a new-born harmonic cycle

- 1: $\phi \leftarrow \hat{\sigma}_i$
 - 2: $\zeta \leftarrow \partial(\hat{\sigma}_i)$
 - 3: **while** $\zeta \neq 0$ and $\exists j$ s.t. $\text{pivot}(\mathbf{BoC}^{p-1}[j]) = \text{pivot}(\zeta)$ **do**
 - 4: $k \leftarrow \text{pivot}(\zeta)$
 - 5: $\alpha_1 \leftarrow \zeta[k]$
 - 6: $\alpha_2 \leftarrow \mathbf{BoC}^{p-1}[j][k]$
 - 7: $\zeta \leftarrow \zeta - (\alpha_1/\alpha_2) \cdot \mathbf{BoC}^{p-1}[j]$
 - 8: $\phi \leftarrow \phi - (\alpha_1/\alpha_2) \cdot \mathbf{Cob}^p[j]$
-

Remark 23. So far we have performed analogous operations on \mathbf{R}^{p-1} and \mathbf{BoC}^{p-1} . However, we notice that \mathbf{R}^{p-1} and \mathbf{BoC}^{p-1} are in general two different matrices with different purposes. The main purpose of \mathbf{R}^{p-1} is to form a filtered basis for $(p-1)$ -boundary groups of complexes in F . Columns in \mathbf{R}^{p-1} are fixed once added to \mathbf{R}^{p-1} . On the other hand, \mathbf{BoC}^{p-1} is mainly for finding a new-born harmonic cycle when σ_i is positive. Columns in \mathbf{BoC}^{p-1} are not fixed and can be changed in later steps (such as in Algorithm 4).

Proposition 24. If Algorithm 3 ends with $\zeta = 0$, then σ_i is positive and ϕ is a new harmonic p -cycle born in $\mathbb{H}_p(K_{i+1})$; otherwise, σ_i is negative.

Proof. Since $\hat{\sigma}_i$ is a new p -cocycle in K_{i+1} , we have that ϕ is always a new p -cocycle in K_{i+1} and $\zeta = \partial(\phi)$ at the end of each iteration in Algorithm 3. If Algorithm 3 ends with $\zeta = 0$, then we have $\partial(\phi) = 0$. This implies that ϕ is a new harmonic p -cycle born in $\mathbb{H}_p(K_{i+1})$. By Theorem 7, σ_i is positive.

Now consider the case that Algorithm 3 ends with $\zeta \neq 0$. For contradiction, suppose instead that σ_i is positive, and let ψ be a new harmonic p -cycle born in $\mathbb{H}_p(K_{i+1})$. Since columns in \mathbb{H}^p and \mathbf{Cob}^p form a basis of $Z^p(K_i)$ and $\hat{\sigma}_i$ is a new p -cocycle in K_{i+1} , we have that \mathbb{H}^p , \mathbf{Cob}^p , and $\hat{\sigma}_i$ altogether form a basis of $Z^p(K_{i+1})$. Hence, we have

$$\psi = \alpha \cdot \hat{\sigma}_i + \sum_j \mu_j \cdot \mathbb{H}^p[j] + \sum_k \lambda_k \cdot \mathbf{Cob}^p[k],$$

where $\alpha \neq 0$ because ψ is a new p -cocycle in K_{i+1} . So we have

$$\begin{aligned} 0 = \partial(\psi) &= \alpha \cdot \partial(\hat{\sigma}_i) + \sum_j \mu_j \cdot \partial(\mathbb{H}^p[j]) + \sum_k \lambda_k \cdot \partial(\mathbf{Cob}^p[k]) \\ &= \alpha \cdot \partial(\hat{\sigma}_i) + 0 + \sum_k \lambda_k \cdot \mathbf{BoC}^{p-1}[k]. \end{aligned}$$

Now

$$\partial(\hat{\sigma}_i) = \sum_k (-\lambda_k/\alpha) \cdot \mathbf{BoC}^{p-1}[k],$$

i.e., $\partial(\hat{\sigma}_i)$ is a linear combination of columns of \mathbf{BoC}^{p-1} . Since the columns of \mathbf{BoC}^{p-1} have distinct pivots, the reduction in Algorithm 3 must end with $\zeta = 0$, which is a contradiction. \square

By Proposition 24, Algorithm 3 must end with $\zeta = 0$ and we add ϕ as new column to \mathbb{H}^p . Now consider the pseudo-cochain

$$\psi_j : B_{p-1}(K_i) \rightarrow \mathbb{R}$$

in K_i that a column $\mathbf{SC}^{p-1}[j]$ encodes. Since $B_{p-1}(K_i) = B_{p-1}(K_{i+1})$ [27, 29], we can directly treat ψ_j as a pseudo-cochain in K_{i+1} . However, while we still have

$$\delta(\psi_j)(\sigma) = \mathbf{Cob}^p[j](\sigma) \text{ for each } p\text{-simplex } \sigma \in K_i,$$

we may have

$$\delta(\psi_j)(\sigma_i) = \psi_j(\partial\sigma_i) \neq 0,$$

so that

$$\mathbf{Cob}^p[j] \neq \delta(\mathbf{SC}^{p-1}[j])$$

in K_{i+1} . To deal with this, we first allocate two new matrices $\overline{\mathbf{Cob}}^p$, $\overline{\mathbf{BoC}}^{p-1}$ and let

$$\overline{\mathbf{Cob}}^p[j] = \delta(\mathbf{SC}^{p-1}[j]) := \delta(\psi_j), \quad \overline{\mathbf{BoC}}^{p-1}[j] = \partial(\overline{\mathbf{Cob}}^p[j]) \text{ for each } j,$$

where all the chains and (pseudo-)cochains are now defined in K_{i+1} . To get $\overline{\mathbf{Cob}}^p[j]$, we only need to know the value of $\psi_j(\partial\sigma_i)$. From the reduction in Algorithm 2, we know how to express $\partial\sigma_i$ as a formal sum of columns in \mathbf{R}^{p-1} , i.e.,

$$\partial\sigma_i = \sum_k \mu_k \mathbf{R}^{p-1}[k],$$

where each non-zero μ_k is given by the “ α_1/α_2 ” in Algorithm 2. Then,

$$\psi_j(\partial\sigma_i) = \psi_j\left(\sum_k \mu_k \mathbf{R}^{p-1}[k]\right) = \sum_k \mu_k \psi_j(\mathbf{R}^{p-1}[k]) = \sum_k \mu_k \mathbf{SC}[j][k].$$

Due to the previous update, columns in $\overline{\mathbf{BoC}}^{p-1}$ may not have distinct pivots. We then run Algorithm 4 to make columns in $\overline{\mathbf{BoC}}^{p-1}$ have distinct pivots again. To see how Algorithm 4 works, notice that before executing the for loop in line 4, we have

$$\overline{\mathbf{Cob}}^p[\lambda_j] = \mathbf{Cob}^p[\lambda_j] + \alpha_j \hat{\sigma}_i \text{ for } j \in \{1, \dots, \ell\}.$$

This means that

$$\overline{\text{BoC}}^{p-1}[\lambda_j] = \text{BoC}^{p-1}[\lambda_j] + \alpha_j \partial(\hat{\sigma}_i).$$

So for $j > 1$, we have

$$\begin{aligned} & \overline{\text{BoC}}^{p-1}[\lambda_j] - (\alpha_j/\alpha_1) \cdot \overline{\text{BoC}}^{p-1}[\lambda_1] \\ &= \text{BoC}^{p-1}[\lambda_j] + \alpha_j \partial(\hat{\sigma}_i) - (\alpha_j/\alpha_1)(\text{BoC}^{p-1}[\lambda_1] + \alpha_1 \partial(\hat{\sigma}_i)) \\ &= \text{BoC}^{p-1}[\lambda_j] - (\alpha_j/\alpha_1) \cdot \text{BoC}^{p-1}[\lambda_1]. \end{aligned}$$

Since $\text{pivot}(\text{BoC}^{p-1}[\lambda_1]) < \text{pivot}(\text{BoC}^{p-1}[\lambda_j])$, we have

$$\text{pivot}(\overline{\text{BoC}}^{p-1}[\lambda_j]) = \text{pivot}(\text{BoC}^{p-1}[\lambda_j])$$

after executing the for loop. Now we have

$$\overline{\text{BoC}}^{p-1}[\lambda] = \text{BoC}^{p-1}[\lambda] \text{ for } \lambda \notin \{\lambda_1, \dots, \lambda_\ell\},$$

meaning that before executing the while loop in line 9, only pivots of the two columns indexed by λ_1 may differ in $\overline{\text{BoC}}^{p-1}$ and BoC^{p-1} . This means that at most two columns in $\overline{\text{BoC}}^{p-1}$ may have the same pivot before executing the while loop. We then have that, in each iteration of the while loop, at most two columns in $\overline{\text{BoC}}^{p-1}$ have the same pivot. Hence, columns in $\overline{\text{BoC}}^{p-1}$ have distinct pivots after finishing the loop. Notice that the pivot k in line 10 decreases in each iteration, meaning that the while loop executes for no more than i iterations. Hence, Algorithm 4 runs in $O(m^2)$ time. Notice that allocating the two new matrices $\overline{\text{Cob}}^p, \overline{\text{BoC}}^{p-1}$ are purely for clearly presenting and justifying the operations in Algorithm 4. To implement this in computer, the operations can be directly performed on Cob^p and BoC^{p-1} .

Algorithm 4 Making columns in $\overline{\text{BoC}}^{p-1}$ have distinct pivots

- 1: let $\overline{\text{Cob}}^p[\lambda_1], \dots, \overline{\text{Cob}}^p[\lambda_\ell]$ be all the columns in $\overline{\text{Cob}}^p$ s.t. $\overline{\text{Cob}}^p[\lambda_j](\sigma_i) \neq 0$ for each j
 - 2: reorder $\lambda_1, \dots, \lambda_\ell$ s.t. $\text{pivot}(\text{BoC}^{p-1}[\lambda_1]) < \text{pivot}(\text{BoC}^{p-1}[\lambda_j])$ for each $j > 1$
 - 3: $\alpha_1 \leftarrow \overline{\text{Cob}}^p[\lambda_1](\sigma_i)$
 - 4: **for** $j = 2, \dots, \ell$ **do**
 - 5: $\alpha_j \leftarrow \overline{\text{Cob}}^p[\lambda_j](\sigma_i)$
 - 6: $\text{SC}^{p-1}[\lambda_j] \leftarrow \text{SC}^{p-1}[\lambda_j] - (\alpha_j/\alpha_1) \cdot \text{SC}^{p-1}[\lambda_1]$
 - 7: $\overline{\text{Cob}}^p[\lambda_j] \leftarrow \overline{\text{Cob}}^p[\lambda_j] - (\alpha_j/\alpha_1) \cdot \overline{\text{Cob}}^p[\lambda_1]$
 - 8: $\overline{\text{BoC}}^{p-1}[\lambda_j] \leftarrow \overline{\text{BoC}}^{p-1}[\lambda_j] - (\alpha_j/\alpha_1) \cdot \overline{\text{BoC}}^{p-1}[\lambda_1]$
 - 9: **while** exist two columns $\overline{\text{BoC}}^{p-1}[\lambda], \overline{\text{BoC}}^{p-1}[\mu]$ with same pivot **do**
 - 10: $k \leftarrow \text{pivot}(\text{BoC}^{p-1}[\lambda])$
 - 11: $\gamma_1 \leftarrow \text{BoC}^{p-1}[\lambda][k]$
 - 12: $\gamma_2 \leftarrow \text{BoC}^{p-1}[\mu][k]$
 - 13: $\text{SC}^{p-1}[\lambda] \leftarrow \text{SC}^{p-1}[\lambda] - (\gamma_1/\gamma_2) \cdot \text{SC}^{p-1}[\mu]$
 - 14: $\overline{\text{Cob}}^p[\lambda] \leftarrow \overline{\text{Cob}}^p[\lambda] - (\gamma_1/\gamma_2) \cdot \overline{\text{Cob}}^p[\mu]$
 - 15: $\overline{\text{BoC}}^{p-1}[\lambda] \leftarrow \overline{\text{BoC}}^{p-1}[\lambda] - (\gamma_1/\gamma_2) \cdot \overline{\text{BoC}}^{p-1}[\mu]$
 - 16: $\text{Cob}^p \leftarrow \overline{\text{Cob}}^p$
 - 17: $\text{BoC}^{p-1} \leftarrow \overline{\text{BoC}}^{p-1}$
-

Finally, we have that the other matrices do not need to be changed by Proposition 16.

σ_i **is negative.** First update \mathbb{H}^{p-1} according to Algorithm 1. Since σ_i is negative, we have $z \neq 0$ at the end of Algorithm 2. We then add z to \mathbb{R}^{p-1} to form a basis for $B_{p-1}(K_{i+1})$ (see [27, 29]). For ease of presentation, let \mathbb{R}^{p-1} still denote the matrix before z is added and let $\overline{\mathbb{R}}^{p-1} = \mathbb{R}^{p-1} \cup \{z\}$. We extend each column of SC^{p-1} by appending 0 so that columns of SC^{p-1} encode $(p-1)$ -pseudo-cochains in K_{i+1} w.r.t $\overline{\mathbb{R}}^{p-1}$. Notice that we may also have $\delta(\text{SC}^{p-1}[j])(\sigma_i) \neq 0$ for a j . Hence, we update Cob^p and BoC^{p-1} as in the previous case where σ_i is positive, including performing Algorithm 4. After this, $\text{Cob}^p[j] = \delta(\text{SC}^{p-1}[j])$, $\text{BoC}^{p-1}[j] = \partial(\text{Cob}^p[j])$ in K_{i+1} for each j and columns in BoC^{p-1} have distinct pivots.

Since $\dim(B^p(K_{i+1})) = \dim(B^p(K_i)) + 1$ by Proposition 16, we need to add a new column to \mathbf{Cob}^p to form a basis for $B^p(K_{i+1})$. For this, we first add the column

$$\vec{v} = (0, \dots, 0, 1)^T$$

to \mathbf{SC}^{p-1} and observe the following:

Proposition 25. Let \vec{v} be as defined above. Then, $\hat{\sigma}_i = \delta(\vec{v})$.

Proof. Let r be the length of \vec{v} and let ψ be the pseudo-cochain encoded by \vec{v} w.r.t $\bar{\mathbf{R}}^{p-1}$. For a p -simplex $\sigma \in K_i$, we have

$$\delta(\vec{v})(\sigma) = \psi(\partial\sigma) = \psi\left(\sum_{k=1}^{r-1} \mu_k \mathbf{R}^{p-1}[k]\right) = \sum_{k=1}^{r-1} \mu_k \psi(\mathbf{R}^{p-1}[k]) = 0.$$

Also, by the reduction in Algorithm 2, we have

$$\partial\sigma_i = \sum_{k=1}^{r-1} \lambda_k \mathbf{R}^{p-1}[k] + z.$$

Then,

$$\delta(\vec{v})(\sigma_i) = \psi(\partial\sigma_i) = \psi\left(\sum_{k=1}^{r-1} \lambda_k \mathbf{R}^{p-1}[k] + z\right) = \psi(z) = 1. \quad \square$$

Proposition 26. The columns in \mathbf{Cob}^p along with $\hat{\sigma}_i$ form a basis for $B^p(K_{i+1})$.

Proof. Abuse the notations slightly by letting \mathbf{Cob}^p and $\overline{\mathbf{Cob}}^p$ denote versions of the two matrices before executing Algorithm 4, i.e., columns in \mathbf{Cob}^p are still cochains in K_i forming a basis of $B^p(K_i)$ and each $\overline{\mathbf{Cob}}^p[j]$ (a cochain in K_{i+1}) is simply derived by taking the coboundary of $\mathbf{SC}^{p-1}[j]$ in K_{i+1} . We first show that columns of $\overline{\mathbf{Cob}}^p[j]$ and $\hat{\sigma}_i$ are linearly independent. Suppose that

$$\sum_j \alpha_j \overline{\mathbf{Cob}}^p[j] + \gamma \hat{\sigma}_i = 0.$$

Let $\iota^\sharp : C^p(K_{i+1}) \rightarrow C^p(K_i)$ be the cochain map induced by inclusion. We have that

$$\sum_j \alpha_j \mathbf{Cob}^p[j] = \sum_j \alpha_j \iota^\sharp(\overline{\mathbf{Cob}}^p[j]) = \iota^\sharp\left(\sum_j \alpha_j \overline{\mathbf{Cob}}^p[j]\right) = \iota^\sharp(-\gamma \hat{\sigma}_i) = -\gamma \iota^\sharp(\hat{\sigma}_i) = 0,$$

meaning that each α_j is zero. This also means that $\gamma = 0$ because $\hat{\sigma}_i \neq 0$. We then have that columns of $\overline{\mathbf{Cob}}^p[j]$ along with $\hat{\sigma}_i$ form a basis of $B^p(K_{i+1})$ because $\hat{\sigma}_i \in B^p(K_{i+1})$ (Proposition 25) and $\dim(B^p(K_{i+1})) = \dim(B^p(K_i)) + 1$ (Proposition 16). Proposition 26 then follows because Algorithm 4 does not change the linear span of matrix columns. \square

By Propositions 25 and 26, we add $\hat{\sigma}_i$ to \mathbf{Cob}^p and add $\partial(\hat{\sigma}_i)$ to \mathbf{BoC}^{p-1} . Notice that there may be at most two columns having the same pivot in \mathbf{BoC}^{p-1} after this. For this, we apply a procedure similar to the while loop in Algorithm 4 to make \mathbf{BoC}^{p-1} have distinct pivots again.

By Proposition 16, the other matrices do not need to be changed.

We now conclude the following:

Theorem 27. The harmonic chain barcode of F can be computed in $O(m^3)$ time.

Proof. Each iteration of the algorithm takes no more than $O(m^2)$ time and so the overall complexity is $O(m^3)$. Correctness of our implementation follows from correctness of the operations detailed in this section. \square

6 Sublevel Set Harmonic Chain Barcode and Its Stability

In this section, we introduce the notion of *sublevel set harmonic chain barcodes* and present our stability results based on this notion. Our stability proof makes use of the work on the algebraic stability of block decomposable \mathbb{R}^2 -modules [1, 6]. In brief, we “lift” the 1-parameter harmonic zigzag module to an \mathbb{R}^2 -indexed 2-parameter persistence module which is block decomposable. We then show that in the typical setting of sublevel set filtrations, there exists an interleaving between the lifted modules. Our main work here is to construct a concrete extension (see Sec. 6.3) and an interleaving between extensions to \mathbb{R}^2 -modules (see Sec. 6.6) realizing the category-theoretic concepts employed in [1, 6]. From the Isometry Theorem [3, 6], we then deduce the stability of the sublevel set harmonic chain barcode. We also address the disparity between the natural harmonic chain barcode of a sublevel set filtration (which consists of closed-open intervals¹) and common conventions of zigzag persistence (which work with closed-closed intervals in our setting).

6.1 Interleaving and Stability for Ordinary Persistence

Let F and G be two filtrations over the complexes K and K' respectively, and let the maps connecting the complexes in F and G be $f^{s,t}$ and $g^{s,t}$ respectively, for $s \leq t \in \mathbb{R}$. Let $C(F)$ and $C(G)$ be the corresponding filtrations of chain groups, and $H(F)$ and $H(G)$ the corresponding persistence modules. With an abuse of notation, we denote the maps induced on chain groups and homology groups also by $f^{s,t}$ and $g^{s,t}$ respectively, where $s \leq t \in \mathbb{R}$.

Definition 28. Let F and G be two filtrations over K and K' respectively. An ε -chain-interleaving between F and G (or an ε -interleaving at the chain level) is given by two sets of homomorphisms $\{\phi_\alpha : C(K_\alpha) \rightarrow C(K'_{\alpha+\varepsilon})\}$ and $\{\psi_\alpha : C(K'_\alpha) \rightarrow C(K_{\alpha+\varepsilon})\}$, such that

1. $\{\phi_\alpha\}$ and $\{\psi_\alpha\}$ commute with the maps in the filtration, that is, for all $\alpha, t \in \mathbb{R}$, $g^{\alpha+\varepsilon, \alpha+\varepsilon+t} \phi_\alpha = \phi_{\alpha+t} f^{\alpha, \alpha+t}$ and $f^{\alpha+\varepsilon, \alpha+\varepsilon+t} \psi_\alpha = \psi_{\alpha+t} g^{\alpha, \alpha+t}$;
2. The following diagrams commute:

$$\begin{array}{ccccc}
 C(K_\alpha) & \xrightarrow{f^{\alpha, \alpha+\varepsilon}} & C(K_{\alpha+\varepsilon}) & \xrightarrow{f^{\alpha+\varepsilon, \alpha+2\varepsilon}} & C(K_{\alpha+2\varepsilon}) \\
 & \searrow \phi_\alpha & & \searrow \phi_{\alpha+\varepsilon} & \\
 & & C(K'_{\alpha+\varepsilon}) & & C(K'_{\alpha+2\varepsilon}) \\
 & \swarrow \psi_\alpha & & \swarrow \psi_{\alpha+\varepsilon} & \\
 C(K'_\alpha) & \xrightarrow{g^{\alpha, \alpha+\varepsilon}} & C(K'_{\alpha+\varepsilon}) & \xrightarrow{g^{\alpha+\varepsilon, \alpha+2\varepsilon}} & C(K'_{\alpha+2\varepsilon})
 \end{array} \tag{5}$$

The *chain interleaving distance* is defined to be

$$d_{CI}(F, G) := \inf\{\varepsilon \geq 0 \mid \text{there exists an } \varepsilon\text{-chain interleaving between } F \text{ and } G\}. \tag{6}$$

We notice that the standard notion of ε -interleaving [14], denoted $d_I(F, G)$, is analogous to our definition above. However, it is defined on the persistence modules $H(F)$ and $H(G)$ on the homology level [14], rather than the filtration of chain groups. Filtrations on the chain level arising from sublevel-sets of a function are ones that interest us in this paper.

We refer to [14] for proof of the following stability theorem for ordinary persistence.

Theorem 29. Let F and G be filtrations defined over (finite) complexes K and K' , respectively. Then

$$d_B(\text{Dgm}(F), \text{Dgm}(G)) \leq d_I(F, G).$$

See [19, 14] for more on the stability of ordinary persistence. We also notice that in the above theorem we can replace d_{CI} in place of d_I , since the existence of an ε -chain-interleaving implies the existence of an ε -interleaving on the homology level.

¹The closed-open intervals over the real values we have here are different from the closed-open intervals of [1, 6] over the integers. Indeed, when considering only integer indices, we only have closed-closed intervals in our setting. The extension of our closed-open interval would be similar to a closed block of [6] but with the right vertical side open.

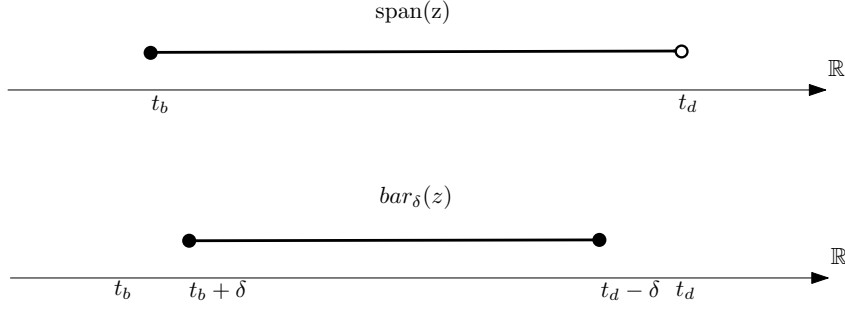


Figure 3: Turning closed-open spans into closed bars

6.2 Sub-level-Set Filtration

Note that we assumed up until now a filtration to be simplex-wise. While this is not true for a sublevel set filtration, we shall construct simplex-wise filtrations from a general filtration.

Definition 30. Let \tilde{F} be an increasing filtration of complex K which is not necessarily simplex-wise and let $z \in Z_p(K)$ be a p -cycle. Let $t_{b(z)}$ be the time when z is born, i.e., $z \in Z_p(K_{t_{b(z)}}) \setminus Z_p(K_{t_{b(z)}-1})$, and $t_{d(z)}$ be the time when z dies as a harmonic chain, i.e., $\delta(z) \neq 0$ in $K_{t_{d(z)}}$, but $\delta(z) = 0$ in K_t for $t_{b(z)} \leq t < t_{d(z)}$. Define the *span* of z as $\text{span}(z) = [t_{b(z)}, t_{d(z)})$. If z is not harmonic at birth, its span is the empty set (notice that a cycle continues to be non-harmonic once it becomes so). The *bar* of z is defined as $\text{bar}(z) := [t_{b(z)}, t_{d(z)}-1]$.

Let \tilde{F} be an increasing filtration of K which is not necessarily simplex-wise, i.e., two consecutive complexes in \tilde{F} can differ by more than one simplex. We fix an ordering, once and for all, for vertices of K , which also fixes an ordering for all K 's simplices (using, say, the lexicographic ordering of the ordered sequence of vertices in a simplex). Given $\delta > 0$ small enough, we expand \tilde{F} into a simplex-wise filtration $\tilde{F}(\delta)$ by expanding each inclusion $K_{t_{i-1}} \hookrightarrow K_{t_i}$ in \tilde{F} starting with $i = 1$. To differentiate, denote each complex in $\tilde{F}(\delta)$ as K'_t where $t \in \mathbb{R}$ is a timestamp. In each iteration, we expand the following inclusion in \tilde{F} :

$$K_{t_{i-1}} \hookrightarrow K_{t_i}$$

into several simplex-wise inclusions in $\tilde{F}(\delta)$:

$$K_{t_{i-1}} = K'_s \hookrightarrow K'_{t_i-\delta} \hookrightarrow K'_{t_i} \hookrightarrow K'_{t_i+\delta} \hookrightarrow \dots \hookrightarrow K'_{t_i+(k-1)\delta} = K_{t_i}.$$

In the above, $K'_{t_i-\delta}$ is a “dummy” complex equal to K'_s (so $K'_s \hookrightarrow K'_{t_i-\delta}$ is an identity map) and k is the number of simplices added from $K_{t_{i-1}}$ to K_{t_i} in \tilde{F} . In short, adding the dummy complexes makes sure that the closed bars of the simplex-wise filtration “induce” the closed-open time intervals in \tilde{F} in which a cycle is harmonic; see Sec. 6 for details. We also have that the k number of simplices are added based on their simplex ordering described above.

Let $\text{span}_\delta(z)$ denote the span of z in $\tilde{F}(\delta)$, and analogously define $\text{bar}_\delta(z)$, $b_\delta(z)$, and $d_\delta(z)$. We observe that addition of dummy complexes implies that for a cycle z , bar of z in $\tilde{F}(\delta)$ must approximate the span of z in \tilde{F} ; see Fig. 3 for an example. In more detail we have the following.

Lemma 31. Let m be the size of K and let $z \in Z_*(K)$ be a cycle. For $\delta > 0$ sufficiently small, $t_{b(z)} \leq t_{b_\delta(z)} \leq t_{b(z)} + m\delta$, and $t_{d(z)} \leq t_{d_\delta(z)} \leq t_{d(z)} + m\delta$. Moreover, we have $t_{d(z)} - \delta \leq t_{d_\delta(z)-1} \leq t_{d(z)} + (m-1)\delta$.

Proof. Since $K_{t_i-\delta} = K_{t_{i-1}}$, we have $b_\delta(z) \geq b(z)$. It is clear that $b_\delta(z) \leq b(z) + m\delta$. The inequalities for $d_\delta(z)$ can also be easily checked.

$t_{d_\delta(z)-1}$ is the largest (real valued) index smaller than $t_{d(z)}$. The smallest that this index can be is the index of a dummy complex added before $K_{t_{d(z)}}$, and the largest it can be is the one to last index among complexes added after $K_{d(z)}$. \square

Therefore, the barcode of $\tilde{F}(\delta)$ can induce a barcode for \tilde{F} . Indeed, for any δ small enough, there is an obvious mapping $\Gamma : \tilde{F}(\delta) \rightarrow \tilde{F}$.

Definition 32. Let F be a simplex-wise filtration (as in Sec. 3.2) and let $\check{\mathbb{B}}^{\mathbb{H}}(F)$ be the *closed-open barcode* of $\mathbb{H}(F)$, i.e., $[t_b, t_d) \in \check{\mathbb{B}}^{\mathbb{H}}(F)$ iff $[t_b, t_{d-1}] \in \mathbb{B}^{\mathbb{H}}(F)$. Moreover, let \tilde{F} and $\tilde{F}(\delta)$ be as defined in this section. We define the *harmonic chain barcode* of \tilde{F} as the set $\check{\mathbb{B}}^{\mathbb{H}}(\tilde{F}) := \Gamma(\check{\mathbb{B}}^{\mathbb{H}}(\tilde{F}(\delta)))$ for δ small enough.

Note that $\check{\mathbb{B}}^{\mathbb{H}}(\tilde{F})$ is the limit of $\mathbb{B}^{\mathbb{H}}(\tilde{F}(\delta))$ as δ approaches 0.

In the rest of this section, we proof stability with respect to simplex-wise filtrations and at the end we show the stability for sublevel set harmonic barcode.

6.3 \mathbb{U} -indexed Persistence Modules

Let \mathbb{R}^{op} denote the poset \mathbb{R} with opposite ordering. Let \mathbb{U} be the subset of $\mathbb{R}^{op} \times \mathbb{R}$ consisting of pairs $(a, b), a \leq b$. Note that $(a, b) < (c, d)$ if and only if $c < a, b < d$. Therefore, \mathbb{U} can be considered as consisting of real-valued intervals with the order being inclusions between the intervals. A *\mathbb{U} -indexed persistence module* M is a functor from the poset \mathbb{U} to the category of vector spaces. We have for each (a, b) , a vector space $M_{(a,b)}$, and for each relation $(a, b) < (c, d)$, a linear map² $f : M_{(a,b)} \rightarrow M_{(c,d)}$.

We now define the *lift* (or *extension*) of the harmonic zigzag module $\mathbb{H}(F)$, denoted $E = E(\mathbb{H}(F))$. We have

$$E(a, b) = \{z \in Z_*(K) \mid b(z) \leq b, d(z) \geq a\}.$$

That is, $E(a, b)$ contains the chains that are born at or before b and die at or after a (see Definition 30). Observe that if z and z' are born at or before t , then $z + z'$ is born at or before t , and if z and z' die at or after t , then $z + z'$ dies at or after t . To see the last statement, let d be the minimum time that z and z' die, and assume $z_1 + z_2$ dies at $t_i < d$. Then $z + z' \notin K_{t_{i+1}} \subset K_{t_i}$. Therefore, one of z and z' must also not be in the image, which is a contradiction. From these observations we deduce the following.

Lemma 33. For any $(a, b) \in \mathbb{U}$, $E(a, b)$ is a vector space.

Lemma 34. The extension operator E respects direct sums.

If $(a, b) < (c, d)$, then $[a, b] \subset [c, d]$ and we have an inclusion $E(a, b) \subset E(c, d)$. These are maps of the extension \mathbb{U} -module. Note that *each* cycle of K is in some $E(a, b)$ where a could be possibly equal to b .

6.4 Blocks and Block-Decomposable Modules

An *interval* in a \mathbb{U} -Module M is a subset $\mathcal{J} \subset \mathbb{U}$ such that

1. \mathcal{J} is non-empty,
2. if $p, q \in \mathcal{J}$ and $p \leq r \leq q$, then $r \in \mathcal{J}$, and,
3. for any $p, q \in \mathcal{J}$, there is a sequence $p = r_0, r_1, \dots, r_l = q$ of elements of \mathcal{J} such that for all $0 \leq j \leq l - 1$, r_j and r_{j+1} are comparable (connectivity).

A multiset of intervals in \mathbb{U} is called a *barcode*.

For \mathcal{J} an interval in \mathbb{U} , the *interval module* $I^{\mathcal{J}}$ is a \mathbb{U} -indexed module such that $I_p^{\mathcal{J}} = \mathbb{R}$ if $p \in \mathcal{J}$, and $I_a^{\mathcal{J}} = 0$ otherwise. The maps satisfy $f : p \rightarrow q = id_{\mathbb{R}}$ if $p \leq q \in \mathcal{J}$ and 0 otherwise.

The intervals for a \mathbb{U} -Module are indecomposable modules analogous to the interval modules in an \mathbb{R} -indexed persistence module [6, Prop. 2.2]. However, contrary to the 1D persistence, a general \mathbb{U} -indexed module cannot be decomposed into interval modules. Note that the harmonic zigzag module is decomposable into interval modules. This implies that the module E is decomposable into special forms of intervals called blocks.

For a closed interval $[a, b] \subset \mathbb{R}^+$ the *closed block* $\mathcal{J}_{BL} = [a, b]_{BL}$ is an interval in \mathbb{U} defined by

$$[a, b]_{BL} = \{(x, y) \in \mathbb{U} \mid x \leq b, y \geq a\}.$$

See Fig. 4. A multiset of blocks in \mathbb{U} is called a *block barcode*.

For any block \mathcal{J}_{BL} , the interval module $I^{\mathcal{J}_{BL}}$ is called a *block module*. A \mathbb{U} -indexed module is *block decomposable* if it can be written as a direct sum of block modules.

It is not difficult to check that if $[a, b]$ is a closed interval for a zigzag module, then $E(a, b)$ is a closed block module. Since the direct sum is preserved by E , we have the following.

²For simplicity we omit the subscripts for maps as long as this does not cause confusions.

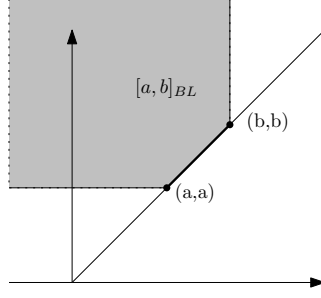


Figure 4: The extension of a closed interval is a closed block.

Lemma 35. The \mathbb{U} -indexed module $E(\mathbb{H}(F))$ is block decomposable.

6.5 Interleaving of \mathbb{U} -Indexed Modules

To define ε -interleaving between \mathbb{U} -indexed modules, we need to first define a *shift operator* S^ε . For a \mathbb{U} -indexed module M , we have a shifted module $S^\varepsilon(M)$ such that $S^\varepsilon(M)_{(a,b)} = M_{(a-\varepsilon, b+\varepsilon)}$, and for $f : M_{(c,d)} \rightarrow M_{(a,b)}$, $S^\varepsilon(f) = f : M_{(c-\varepsilon, d+\varepsilon)} \rightarrow M_{(a-\varepsilon, b+\varepsilon)}$.

Given $\varepsilon \geq 0$, two \mathbb{U} -indexed modules M, N are ε -interleaved if there exist a pair of morphisms $\Phi : M \rightarrow S^\varepsilon(N)$ and $\Psi : N \rightarrow S^\varepsilon(M)$ such that for each $(a, b) \in \mathbb{U}$

$$\Psi_{(a-\varepsilon, b+\varepsilon)} \circ \Phi_{(a,b)} = f : M_{(a,b)} \rightarrow M_{(a-2\varepsilon, b+2\varepsilon)}$$

and

$$\Phi_{(a-\varepsilon, b+\varepsilon)} \circ \Psi_{(a,b)} = g : N_{(a,b)} \rightarrow N_{(a-2\varepsilon, b+2\varepsilon)},$$

where g in the above denotes maps of N .

The *interleaving-distance* between two \mathbb{U} -indexed modules M and N is defined as

$$d_I(M, N) = \inf\{\varepsilon \mid \text{there is an } \varepsilon\text{-interleaving between } M \text{ and } N\}.$$

6.6 Stability of Harmonic Chain Barcode

Let F be a filtration. Define $\rho(F) = \max\{t_{d(z)} - t_{d(z)-1} \mid z \in Z_*(K)\}$, that is, $\rho(F)$ the maximum distortion caused by turning spans into closed bars.

Theorem 36. Let F and G be simplex-wise increasing filtrations where the maps of F and G are inclusions. Assume that the interleaving distance at chain level between F and G is obtained via inclusions. Then

$$d_B(\mathbb{B}^{\mathbb{H}}(F), \mathbb{B}^{\mathbb{H}}(G)) \leq d_I(F, G) + \max\{\rho(F), \rho(G)\}.$$

Proof. Set $M = E(\mathbb{H}(F))$ and $N = E(\mathbb{H}(G))$. Let $\varepsilon = d_I(F, G)$. We define $\Phi_{(a,b)} : M_{(a,b)} \rightarrow N_{(a-\varepsilon-\rho(F), b+\varepsilon+\rho(F))}$ to be the inclusion. Note that Φ is well-defined since all the cycles exist in the extension. The morphism $\Psi = \{\Psi_{(a,b)} \mid (a, b) \in \mathbb{U}\}$ is defined analogously. Since all the maps are inclusions, the morphisms Φ and Ψ define an ε -interleaving of M and N . It follows that $d_I(M, N) \leq \varepsilon + \max\{\rho(F), \rho(G)\}$. From the isometry theorem for block decomposable \mathbb{U} -indexed modules [1, 6], we deduce that $d_B(\mathcal{D}(M), \mathcal{D}(N)) = d_I(M, N) \leq \varepsilon + \max\{\rho(F), \rho(G)\}$, where $\mathcal{D}(M)$ and $\mathcal{D}(N)$ are the block barcodes of M and N respectively. Any matching of block barcodes induces a matching of the parts of the blocks on the diagonal which form the barcodes of the 1D filtrations $\mathbb{H}(F)$ and $\mathbb{H}(G)$ and vice versa ([6, Proposition 4.2]). It follows that $d_B(\mathbb{B}^{\mathbb{H}}(F), \mathbb{B}^{\mathbb{H}}(G)) = d_B(\mathcal{D}(M), \mathcal{D}(N)) \leq \varepsilon + \max\{\rho(F), \rho(G)\}$. \square

Corollary 37. Let $\hat{f}, \hat{g} : |K| \rightarrow \mathbb{R}$ be simplex-wise linear functions, and let \tilde{F} and \tilde{G} be the sublevel set filtrations of \hat{f} and \hat{g} respectively. Then,

$$d_B(\check{\mathbb{B}}^{\mathbb{H}}(\tilde{F}), \check{\mathbb{B}}^{\mathbb{H}}(\tilde{G})) \leq \|\hat{f} - \hat{g}\|_\infty.$$

Proof. Let m be the number of simplices in K . Let $\varepsilon = \|\hat{f} - \hat{g}\|_\infty$. There is an ε -interleaving between the filtration \tilde{F} and \tilde{G} defined by inclusion of sublevel sets [19, 14]. We can choose δ such that $\varepsilon \gg m\delta$. Then there is an $(\varepsilon + m\delta)$ -interleaving between $\tilde{F}(\delta)$ and $\tilde{G}(\delta)$, since $K_t \subset K'_{t+\varepsilon+m\delta}$ and $K'_t \subset K_{t+\varepsilon+m\delta}$, where K_t and K'_t are the complexes of $\tilde{F}(\delta)$ and $\tilde{G}(\delta)$ respectively. Moreover, by lemma 31, $\max\{\rho(F), \rho(G)\} \leq m\delta$. Therefore, for all δ such that $m\delta \ll \varepsilon$, $d_B(\check{B}^{\mathbb{H}}(\tilde{F}(\delta)), \check{B}^{\mathbb{H}}(\tilde{G}(\delta))) \leq \varepsilon + m\delta = \|f - g\|_\infty + m\delta$. Since δ approaches 0 the corollary follows. \square

References

- [1] Håvard Bakke Bjerkevik. On the stability of interval decomposable persistence modules. *Discrete & Computational Geometry*, 66(1):92–121, 2021.
- [2] Saugata Basu and Nathanael Cox. Harmonic persistent homology. In *2021 IEEE 62nd Annual Symposium on Foundations of Computer Science (FOCS)*, pages 1112–1123. IEEE, 2022.
- [3] Ulrich Bauer and Michael Lesnick. Induced matchings of barcodes and the algebraic stability of persistence. In *Proceedings of the thirtieth annual symposium on Computational geometry*, pages 355–364, 2014.
- [4] Paul Bendich, Herbert Edelsbrunner, Dmitriy Morozov, and Amit Patel. Homology and robustness of level and interlevel sets. *Homology, homotopy, and applications*, 15(1):51–72, 2013.
- [5] Glencora Borradaile, William Maxwell, and Amir Nayyeri. Minimum bounded chains and minimum homologous chains in embedded simplicial complexes. In *Proceedings of the 36th International Symposium on Computational Geometry (SoCG 2020)*. Schloss Dagstuhl-Leibniz-Zentrum für Informatik, 2020.
- [6] Magnus Botnan and Michael Lesnick. Algebraic stability of zigzag persistence modules. *Algebraic & geometric topology*, 18(6):3133–3204, 2018.
- [7] Oleksiy Busaryev, Tamal K. Dey, and Yusu Wang. Tracking a generator by persistence. In My T. Thai and Sartaj Sahni, editors, *Computing and Combinatorics*, pages 278–287, 2010.
- [8] Gunnar Carlsson and Vin de Silva. Zigzag persistence. *Foundations of Computational Mathematics*, 10(4):367–405, 2010.
- [9] Gunnar Carlsson, Vin de Silva, and Dmitriy Morozov. Zigzag persistent homology and real-valued functions. In *Proceedings of the 25th Annual Symposium on Computational Geometry*, pages 247–256, 2009.
- [10] Gunnar Carlsson, Afra J. Zomorodian, Anne Collins, and Leonidas J. Guibas. Persistence barcodes for shapes. *Proceedings Eurographs/ACM SIGGRAPH Symposium on Geometry Processing*, pages 124–135, 2004.
- [11] Erin W. Chambers, Jeff Erickson, Kyle Fox, and Amir Nayyeri. Minimum cuts in surface graphs. *SIAM Journal on Computing*, 52(1):156–195, 2023. [arXiv:https://doi.org/10.1137/19M1291820](https://doi.org/10.1137/19M1291820), [doi:10.1137/19M1291820](https://doi.org/10.1137/19M1291820).
- [12] Erin W. Chambers, Jeff Erickson, and Amir Nayyeri. Minimum cuts and shortest homologous cycles. In *Proceedings of the 25th International Symposium on Computational Geometry (SoCG 2009)*. ACM Press, 2009. [doi:10.1145/1542362.1542426](https://doi.org/10.1145/1542362.1542426).
- [13] Erin Wolf Chambers, Salman Parsa, and Hannah Schreiber. On complexity of computing bottleneck and lexicographic optimal cycles in a homology class. In *Proceedings of the 38th International Symposium on Computational Geometry (SoCG)*. Schloss Dagstuhl-Leibniz-Zentrum für Informatik, 2022.
- [14] Frédéric Chazal, David Cohen-Steiner, Marc Glisse, Leonidas J. Guibas, and Steve Y. Oudot. Proximity of persistence modules and their diagrams. In *25th Annual Symposium on Computational Geometry (SoCG 2009)*, pages 237–246, New York, NY, USA, 2009. Association for Computing Machinery. [doi:https://doi.org/10.1145/1542362.1542407](https://doi.org/10.1145/1542362.1542407).

- [15] Frédéric Chazal, Vin De Silva, Marc Glisse, and Steve Oudot. *The Structure and Stability of Persistence Modules*, volume 10. Springer, 2016.
- [16] Chao Chen and Daniel Freedman. Measuring and computing natural generators for homology groups. *Computational Geometry*, 43(2):169–181, 2010. Special Issue on the 24th European Workshop on Computational Geometry (EuroCG’08). doi:10.1016/j.comgeo.2009.06.004.
- [17] Chao Chen and Daniel Freedman. Hardness results for homology localization. *Discrete & Computational Geometry*, 45(3):425–448, 2011.
- [18] Jiahui Chen, Yuchi Qiu, Rui Wang, and Guo-Wei Wei. Persistent Laplacian projected Omicron BA. 4 and BA. 5 to become new dominating variants. *Computers in Biology and Medicine*, 151:106262, 2022.
- [19] David Cohen-Steiner, Herbert Edelsbrunner, and John Harer. Stability of persistence diagrams. In *Proceedings of the 21st Annual Symposium on Computational Geometry*, pages 263–271, 2005.
- [20] David Cohen-Steiner, Herbert Edelsbrunner, and Dmitriy Morozov. Vines and vineyards by updating persistence in linear time. In *Proceedings of the Twenty-Second Annual Symposium on Computational Geometry*, pages 119–126, 2006.
- [21] Alessandro De Gregorio, Marco Guerra, Sara Scaramuccia, and Francesco Vaccarino. Parallel decomposition of persistence modules through interval bases. *arXiv preprint arXiv:2106.11884*, 2021.
- [22] Vin De Silva, Dmitriy Morozov, and Mikael Vejdemo-Johansson. Persistent cohomology and circular coordinates. *Discrete & Computational Geometry*, 45(4):737–759, 2011.
- [23] Tamal K. Dey, Anil N. Hirani, and Bala Krishnamoorthy. Optimal homologous cycles, total unimodularity, and linear programming. In *Proceedings of the 42nd ACM Symposium on Theory of Computing*, pages 221–230, 2010. doi:10.1145/1806689.1806721.
- [24] Tamal K. Dey and Tao Hou. Computing zigzag persistence on graphs in near-linear time. In *37th International Symposium on Computational Geometry*, 2021.
- [25] Tamal K Dey, Tao Hou, and Sayan Mandal. Computing minimal persistent cycles: Polynomial and hard cases. In *Proceedings of the 14th Annual ACM-SIAM Symposium on Discrete Algorithms*, pages 2587–2606. SIAM, 2020.
- [26] Tamal K. Dey, Tao Hou, and Dmitriy Morozov. A fast algorithm for computing zigzag representatives. *ACM-SIAM Symposium on Discrete Algorithms (SODA) 2025*, to appear.
- [27] Tamal Krishna Dey and Yusu Wang. *Computational Topology for Data Analysis*. Cambridge University Press, 2022.
- [28] Beno Eckmann. Harmonische Funktionen und Randwertaufgaben in einem Komplex. *Commentarii Mathematici Helvetici*, 17(1):240–255, 1944.
- [29] Edelsbrunner, Letscher, and Zomorodian. Topological persistence and simplification. *Discrete & Computational Geometry*, 28:511–533, 2002.
- [30] Herbert Edelsbrunner and John Harer. *Computational Topology: An Introduction*. Applied Mathematics. American Mathematical Society, 2010.
- [31] Robert Ghrist. Barcodes: The persistent topology of data. *Bulletin of the American Mathematical Society*, 45:61–75, 2008.
- [32] Joshua A. Grochow and Jamie Tucker-Foltz. Computational topology and the unique games conjecture. In *Proceedings of 34th International Symposium on Computational Geometry (SoCG 2018)*. Schloss Dagstuhl-Leibniz-Zentrum fuer Informatik, 2018.
- [33] Nicola Guglielmi, Anton Savostianov, and Francesco Tudisco. Quantifying the structural stability of simplicial homology. *arXiv preprint arXiv:2301.03627*, 2023.

- [34] Aziz Burak Gülen, Facundo Mémoli, and Zhengchao Wan. Orthogonal Möbius inversion and Grassmannian persistence diagrams. *arXiv preprint arXiv:2311.06870*, 2024.
- [35] Davide Gurnari, Aldo Guzmán-Sáenz, Filippo Utro, Aritra Bose, Saugata Basu, and Laxmi Parida. Probing omics data via harmonic persistent homology. *arXiv preprint arXiv:2311.06357*, 2023.
- [36] Allen Hatcher. *Algebraic Topology*. Cambridge University Press, 2002.
- [37] Yasuaki Hiraoka, Takenobu Nakamura, Akihiko Hirata, Emerson G Escobar, Kaname Matsue, and Yasumasa Nishiura. Hierarchical structures of amorphous solids characterized by persistent homology. *Proceedings of the National Academy of Sciences*, 113(26):7035–7040, 2016.
- [38] Danijela Horak and Jürgen Jost. Spectra of combinatorial Laplace operators on simplicial complexes. *Advances in Mathematics*, 244:303–336, 2013.
- [39] Alexandros Keros and Kartic Subr. Spectral coarsening with Hodge Laplacians. In *ACM SIGGRAPH 2023 Conference Proceedings*, pages 1–11, 2023.
- [40] G. Kirchhoff. Ueber die Auflösung der Gleichungen, auf welche man bei der Untersuchung der linearen Vertheilung galvanischer Ströme geführt wird. *Annalen der Physik*, 148(12):497–508, 1847. doi:10.1002/andp.18471481202.
- [41] Hyekeyoung Lee, Moo K Chung, Hongyoon Choi, Hyejin Kang, Seunggyun Ha, Yu Kyeong Kim, and Dong Soo Lee. Harmonic holes as the submodules of brain network and network dissimilarity. In *Computational Topology in Image Context: 7th International Workshop, CTIC 2019, Málaga, Spain, January 24-25, 2019, Proceedings 7*, pages 110–122. Springer, 2019.
- [42] Mao Li, Keith Duncan, Christopher N. Topp, and Daniel H. Chitwood. Persistent homology and the branching topologies of plants. *American Journal of Botany*, 104(3):349–353, 2017.
- [43] Andre Lieutier. Persistent harmonic forms. <https://project.inria.fr/gudhi/files/2014/10/Persistent-Harmonic-Forms.pdf>.
- [44] Jian Liu, Jingyan Li, and Jie Wu. The algebraic stability for persistent Laplacians. *arXiv preprint arXiv:2302.03902*, 2023.
- [45] Jiajie Luo and Gregory Henselman-Petrusek. Interval decomposition for persistence modules freely generated over PIDs. *arXiv preprint arXiv:2310.07971*, 2023.
- [46] Clément Maria and Steve Y. Oudot. Zigzag persistence via reflections and transpositions. In Piotr Indyk, editor, *Proceedings of the Twenty-Sixth Annual ACM-SIAM Symposium on Discrete Algorithms, SODA 2015, San Diego, CA, USA, January 4-6, 2015*, pages 181–199. SIAM, 2015.
- [47] Facundo Mémoli, Zhengchao Wan, and Yusu Wang. Persistent Laplacians: Properties, algorithms and implications. *SIAM Journal on Mathematics of Data Science*, 4(2):858–884, 2022.
- [48] Russell Merris. Laplacian matrices of graphs: a survey. *Linear Algebra and its Applications*, 197-198:143–176, 1994. doi:10.1016/0024-3795(94)90486-3.
- [49] Joshua Mike and Jose Perea. Multiscale geometric data analysis via Laplacian eigenvector cascading. In *2019 18th IEEE International Conference On Machine Learning And Applications (ICMLA)*, pages 1091–1098. IEEE, 2019.
- [50] Bojan Mohar, Y Alavi, G Chartrand, and OR Oellermann. The Laplacian spectrum of graphs. *Graph theory, combinatorics, and applications*, 2(871-898):12, 1991.
- [51] Ipei Obayashi. Volume-optimal cycle: Tightest representative cycle of a generator in persistent homology. *SIAM Journal on Applied Algebra and Geometry*, 2(4):508–534, 2018. doi:10.1137/17M1159439.
- [52] Rui Wang, Duc Duy Nguyen, and Guo-Wei Wei. Persistent spectral graph. *International journal for numerical methods in biomedical engineering*, 36(9):e3376, 2020.
- [53] Afra J Zomorodian. *Topology for computing*, volume 16. Cambridge university press, 2005.

A Homology and Cohomology

Let K be a simplicial complex and we give the standard orientation to simplices in K . We write simplices as an ordered set of vertices, e.g., $\sigma = v_0 v_1 \cdots v_p$ for a p -dimensional simplex, for any integer $p \geq 0$. Let K_p denote the set of p -simplices of K and $n_p = |K_p|$. The p -dimensional *chain group* of K with coefficients in \mathbb{R} , denoted $C_p(K)$, is an \mathbb{R} -vector space generated by K_p . By fixing an ordering of the set K_p , we can identify any p -chain $c \in C_p(K)$ with an ordered n_p -tuple with real entries (e.g., an element of \mathbb{R}^{n_p}). For each p , we fix an ordering for the p -simplices once and for all, and identify $C_p(K)$ and \mathbb{R}^{n_p} . The standard basis of \mathbb{R}^{n_p} corresponds (under the identification) to the basis of $C_p(K)$ given by the simplices with standard orientation.

The p -dimensional boundary matrix $\partial_p : C_p(K) \rightarrow C_{p-1}(K)$ is defined on a simplex basis element by the formula

$$\partial(v_0 v_1 \cdots v_p) = \sum_{j=0}^p (-1)^j (v_0 \cdots v_{j-1} v_{j+1} \cdots v_p).$$

In the right hand side above, in the j -th term v_j is dropped. The formula guarantees the crucial property of the boundary homomorphism: $\partial_p \partial_{p+1} = 0$. This simply means that the boundary of a simplex has no boundary. The sequence $C_p(K)$ together with the maps ∂_p define the *simplicial chain complex* of K with real coefficients, denoted $C_\bullet(K)$. The group of p -dimensional *cycles*, denoted $Z_p(K)$, is the kernel of ∂_p . The group of p -dimensional *boundaries*, denoted $B_p(K)$, is the image of ∂_{p+1} . The p -dimensional homology group of K , denoted $H_p(K)$, is the quotient group $Z_p(K)/B_p(K)$. As a set, this quotient is formally defined as $\{z + B_p(K) \mid z \in Z_p(K)\}$. The operations are inherited from the chain group. In words, the homology group is obtained from $Z_p(K)$ by setting any two cycles which differ by a boundary to be equal. All these groups are \mathbb{R} -vector spaces.

Consider the space \mathbb{R}^{n_p} . The cycle group $Z_p(K) \subset C_p(K) = \mathbb{R}^{n_p}$ is a subspace, that is, a hyperplane passing through the origin. Similarly, the boundary group $B_p(K)$ is a subspace, and is included in $Z_p(K)$. The homology group is the set of parallels of $B_p(K)$ inside $Z_p(K)$. Each such parallel hyperplane differs from $B_p(K)$ by a translation given by some cycle z . These parallel hyperplanes partition $Z_p(K)$. The homology group is then isomorphic to the subspace perpendicular to $B_p(K)$ inside $Z_p(K)$. The dimension of the p -dimensional homology group is called the p -th \mathbb{R} -Betti number, denoted $\beta_p(K)$.

Simplicial cohomology with coefficients in \mathbb{R} is usually defined by the process of dualizing. This means that we replace an p -chain by a linear functional $C_p(K) \rightarrow \mathbb{R}$, called a p -dimensional *cochain*. The set of all such linear functionals is a vector space isomorphic to $C_p(K)$, called the cochain group, denoted $C^p(K)$, which is a dual vector space of $C_p(K)$. For the purposes of defining harmonic chains, we must fix an isomorphism. We take the isomorphism that sends each standard basis element of \mathbb{R}^{n_p} , corresponding to σ , to a functional that assigns 1 to σ and 0 to other basis elements, denoted $\hat{\sigma} \in C^p(K)$. Any cochain $\gamma \in C^p(K)$ can be written as a linear combination of the $\hat{\sigma}$. Therefore, it is also a vector in \mathbb{R}^{n_p} . The fixed isomorphism allows us to identify C^p with \mathbb{R}^{n_p} , and hence to C_p . Therefore, any vector in \mathbb{R}^{n_p} is at the same time a chain and a cochain.

The *coboundary matrix* $\delta^p : C^p(K) \rightarrow C^{p+1}(K)$, in its matrix representation, is the transpose of ∂_{p+1} , $\delta^p = \partial_{p+1}^\top$. It follows that $\delta_{p+1} \delta^p = 0$, and we can form a *cochain complex* $C^\bullet(K)$. The group of p -*cocycles*, denoted Z^p is the kernel of δ^p . The group of p -*coboundary* is the image of δ_{p-1} . The p -dimensional *cohomology group*, denoted $H^p(K)$, is defined as $H^p(K) = Z^p(K)/B^p(K)$. All of these groups are again vector subspaces of $C^p(K)$ and thus of \mathbb{R}^{n_p} . It is a standard fact that homology and cohomology groups with real coefficients are isomorphic.

B Justification for the Definition of Harmonic Representatives

Consider a zigzag module $\mathcal{M} : V_0 \xleftarrow{g_0} V_1 \xleftarrow{g_1} \cdots \xleftarrow{g_{k-1}} V_k$ which is *elementary* in the sense that each g_i is either an isomorphism, an injection with corank 1, or a surjection with nullity 1. Representatives for intervals in $\mathbf{B}(\mathcal{M})$ are defined as follows:

Definition 38 (Zigzag representatives [46]). A *representative* for $[b, d] \in \mathbf{B}(\mathcal{M})$ is a sequence $\{v_i \in V_i \mid i \in [b, d]\}$ such that for every $b \leq i < d$, either $g_i(v_i) = v_{i+1}$ or $g_i(v_{i+1}) = v_i$ based on the direction of g_i . Furthermore, we have:

Birth condition: If $g_{b-1} : V_{b-1} \rightarrow V_b$ is forward (thus being injective), $v_b \notin \text{img}(g_{b-1})$; if $g_{b-1} : V_{b-1} \leftarrow V_b$ is backward (thus being surjective), then v_b is the non-zero element in $\ker(g_{b-1})$.

Death condition: If $d < k$ and $g_d : V_d \leftarrow V_{d+1}$ is backward (thus being injective), $v_d \notin \text{img}(g_d)$; if $d < i$ and $g_d : V_d \rightarrow V_{d+1}$ is forward (thus being surjective), then v_d is the non-zero element in $\ker(g_d)$.

Proof of Proposition 10. Let $[b, d]$ be an interval in $\mathbf{B}^{\mathbb{H}}(F) = \mathbf{B}(\mathbb{H}_*(F))$ and let $\{z_i \in \mathbb{H}_*(K_i) \mid i \in [b, d]\}$ be a sequence of representatives for $[b, d]$ as in Definition 38. For each $i < d$, we have that z_i maps to z_{i+1} or z_{i+1} maps to z_i by the inclusion, and hence $z_i = z_{i+1}$. Therefore, the representative $\{z_i \in \mathbb{H}_*(K_i) \mid i \in [b, d]\}$ indeed consists of a single cycle. \square

To see that Definition 11 is an adaption of Definition 38 to the module $\mathbb{H}_p(F)$, we only need to check the birth and death conditions. Let $[b, d]$ be an interval in $\mathbf{B}_p^{\mathbb{H}}(F)$ with a representative z . For the birth condition, since inclusion maps have trivial kernels, we have that z is not in the image of the inclusion $\mathbb{H}_p(K_{b-1}) \hookrightarrow \mathbb{H}_p(K_b)$ by Definition 38. This means that $z \in \mathbb{H}_p(K_b) \setminus \mathbb{H}_p(K_{b-1})$ which is as stated in Definition 11. The death condition can also be similarly verified.

C Justification for \mathbb{H}^p Forming a Basis for $\mathbb{H}_p(K_i)$

We first have the following proposition which follows directly from definitions:

Proposition 39. For a K_i in F , let $\{[b_j, d_j] \mid j \in J\}$ be all the intervals in $\mathbf{B}_p^{\mathbb{H}}(F)$ containing i , where each $[b_j, d_j]$ has a harmonic representative z_j . Then $\{z_j \mid j \in J\}$ forms a basis for $\mathbb{H}_p(K_i)$.

Define a *prefix* F_i of F as the filtration $F_i : K_0 \hookrightarrow K_1 \hookrightarrow \dots \hookrightarrow K_i$. It is then not hard to see the following fact concerning Algorithm 1:

Proposition 40. Before each iteration i processing $K_i \hookrightarrow K_{i+1}$, $\{[b, i] \mid b \in U^p\}$ is the set of all intervals containing i in $\mathbf{B}_p^{\mathbb{H}}(F_i)$ and each partial representative for b maintained by the algorithm is indeed a harmonic representative for $[b, i] \in \mathbf{B}_p^{\mathbb{H}}(F_i)$.

Combining Propositions 39 and 40, we have that columns in \mathbb{H}^p form a basis for $\mathbb{H}_p(K_i)$.